

Wave energy Part 2

Wave energy absorption

OCEN4007 Ocean Renewable Energy

Adi Kurniawan
adi.kurniawan@uwa.edu.au

In Part 1, we looked at the wave energy resource, where we considered briefly how ocean waves are generated, how to calculate the wave-power level of regular and irregular waves, how to calculate the mean wave-power level at a given site, and where we also considered the global distribution of wave-power resource and its variability. In passing, we also looked at the group velocity and the role it plays in wave energy propagation.

In this part, we will mainly consider the fundamental principles of wave energy absorption, but let us first begin by considering some advantages of wave energy and a brief history of the field.

1 What makes wave energy attractive

What makes wave energy attractive? Here are some reasons:

- Wave energy is more *persistent* (less intermittent) than wind or solar energy. As mentioned in Part 1, waves in deep water and open ocean can travel over long distances almost without energy loss. At a given location there may be swells even when there is no wind.
- Wave has a higher energy intensity than solar or wind (see Part 1 for how much denser wave energy is compared to wind and solar).
- The potential is enormous. Globally, it is estimated that there is enough wave energy to provide the electricity needs of about 1 billion homes.
- Wave energy converters (WECs) can act as coastal protection, because they absorb energy from the waves that pass through them. Hence, waves in the lee of WECs carry less energy than the waves before them.
- Minimal visual intrusion. Most WECs do not extend far above the sea surface. Some of them are completely submerged.

2 Brief history of wave energy

The history of wave energy is relatively short compared to that of wind energy. The first known wave energy patent dates back to 1799, a time when windmills, which are not very different in principle from modern wind turbines we see today, were already widespread.

Around 1900s, devices to harness wave energy used to be called wave motors. Some of these were actually built and deployed, but little is known about their fate.

In 1947, the Japanese inventor Yoshio Masuda began testing wave energy devices in Japan. He proposed a number of concepts, some of which still persist in different variants today. At about the same time, Walton Bott began working on wave energy in Mauritius. The scheme he proposed was the precursor of overtopping devices.

In 1965, Ryokuseisha, a Japanese company, began manufacturing wave-powered navigation buoys. This company is still in operation today.

Wave energy received a greater attention in the 1970s. The 1973 oil crisis motivated serious research and development into alternative energy sources, including wave energy. At the University of Edinburgh, Stephen Salter experimented with various shapes in a wave flume and ended up with a shape looking like a nodding duck. He was able to demonstrate, for the first time, that near complete wave absorption is possible.

As a response to the oil crisis, the UK government initiated the UK Wave Power Programme, and a number of devices were deemed promising. These include the Salter Duck, the NEL oscillating water column (OWC), the Lancaster flexible bag, the Bristol cylinder, the Vickers device, and the Clam. Some other notable devices were proposed around this time, including the Cockerell raft (see Fig. 1), which was invented by Sir Christopher Cockerell, the inventor of the hovercraft, the Russell rectifier (see Fig. 1), the Kaimei, and the Triplate. Meanwhile, in Norway, Kjell Budal and Johannes Falnes were experimenting with point absorbers, devices of much smaller extents than typical wavelengths.

As the oil price declined, however, the UK Wave Power Programme was terminated. Devices that were so close to being put to sea were abandoned. Similar situation happened in other countries. Funding for wave energy research was drastically cut. Nevertheless, this period saw the construction of two full-scale plants in Norway: the tapered channel and the Kvaerner OWC (see Fig. 2). Both operated for a few years before being damaged during a severe winter storm.

Wave energy entered a period of relative inactivity which lasted for about two decades, from early 1980s to late 1990s. At the turn of the millennium, research activities in wave energy picked up again, along with increasing awareness of the negative consequences of fossil fuels. A number of devices were tested at sea during this period, including the PowerBuoy, Pelamis, Wavebob, Limpet, Wavestar, Wave Dragon, Oyster, and Seabased, to name a few.

More recent developments include the establishment of [Wave Energy Scotland](#) to reformulate the approach to wave energy development using a stage-gated model and a competitive Pre-Commercial Procurement (PCP) program. This ensures that only the best of the competing concepts get funded and progress to the next stage of development. This model is now followed by the [EuropeWave](#) program.

A summary of important events in wave energy history is presented in the form of a timeline in Fig. 3. As of today, there is no convergence yet in wave energy technology.

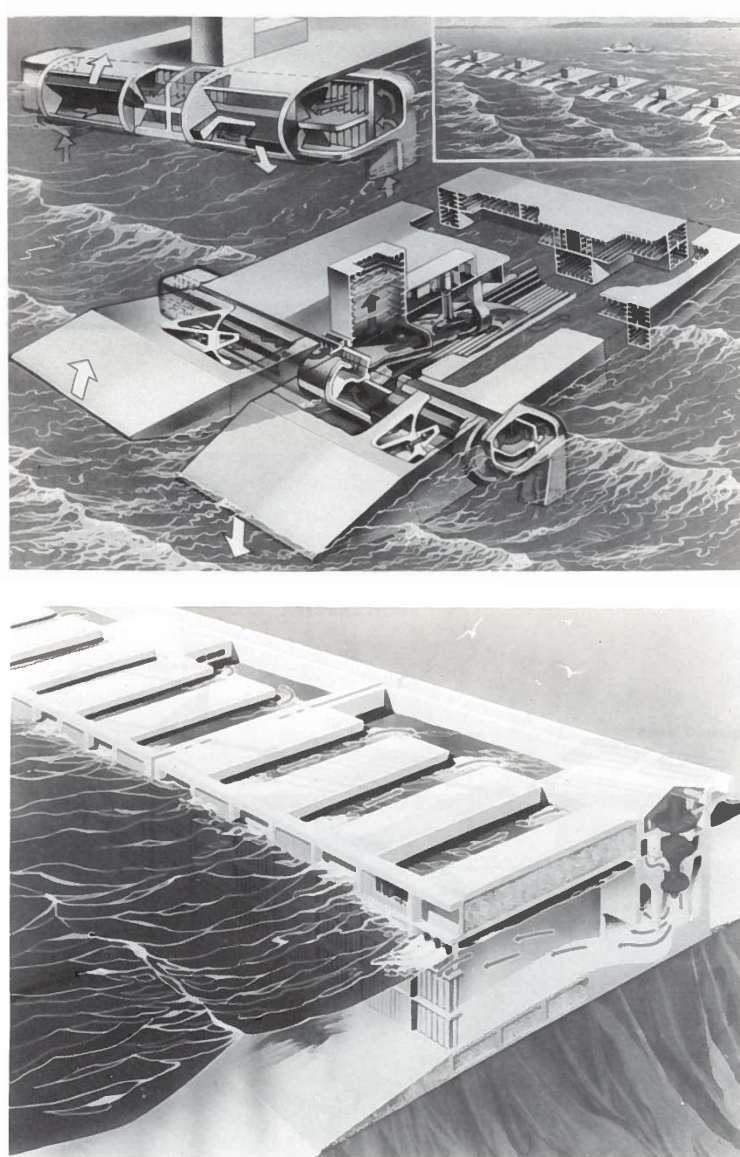


FIGURE 1: The Cockerell raft (top) and the Russell rectifier (bottom), reproduced from [5].

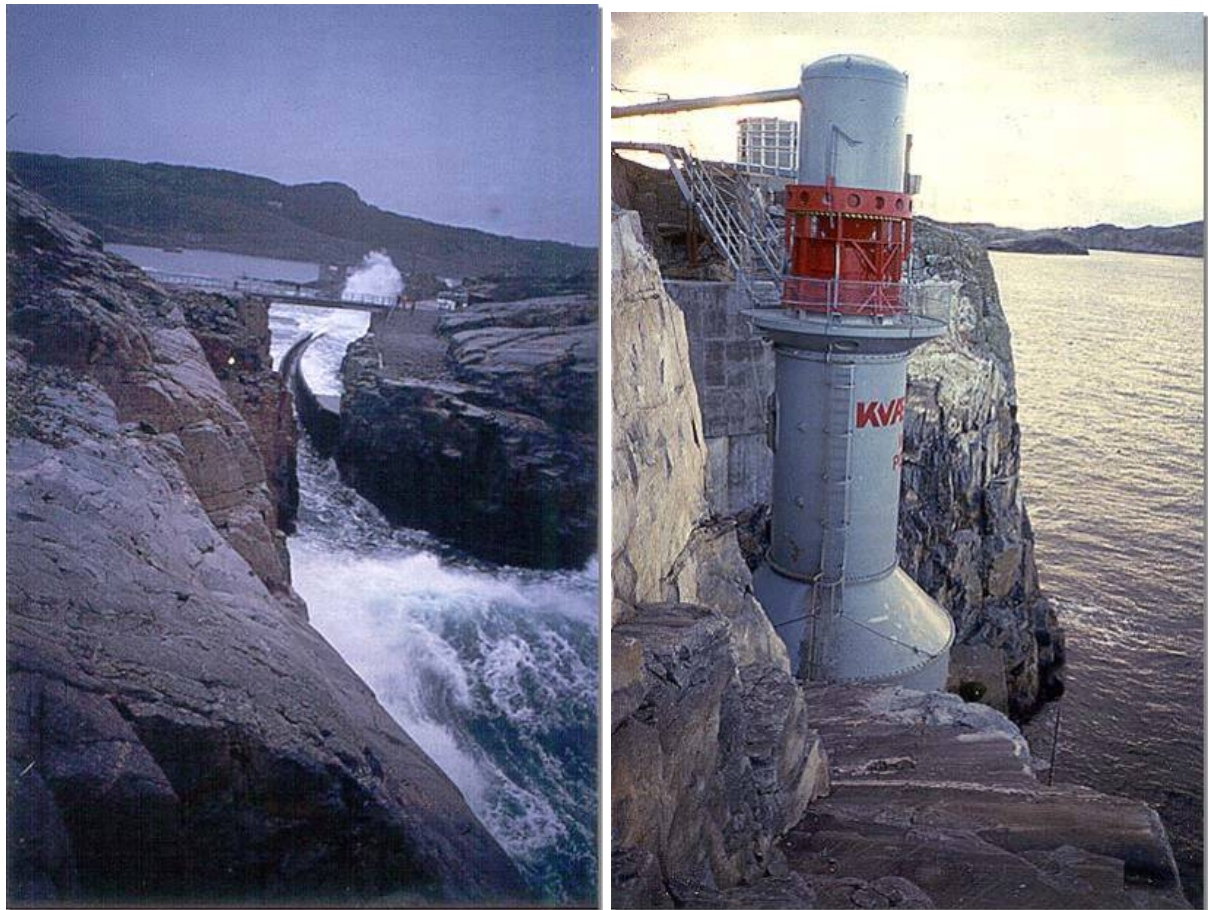


FIGURE 2: The tapered channel (left) and the Kvaerner oscillating water column (right), reproduced from [3].

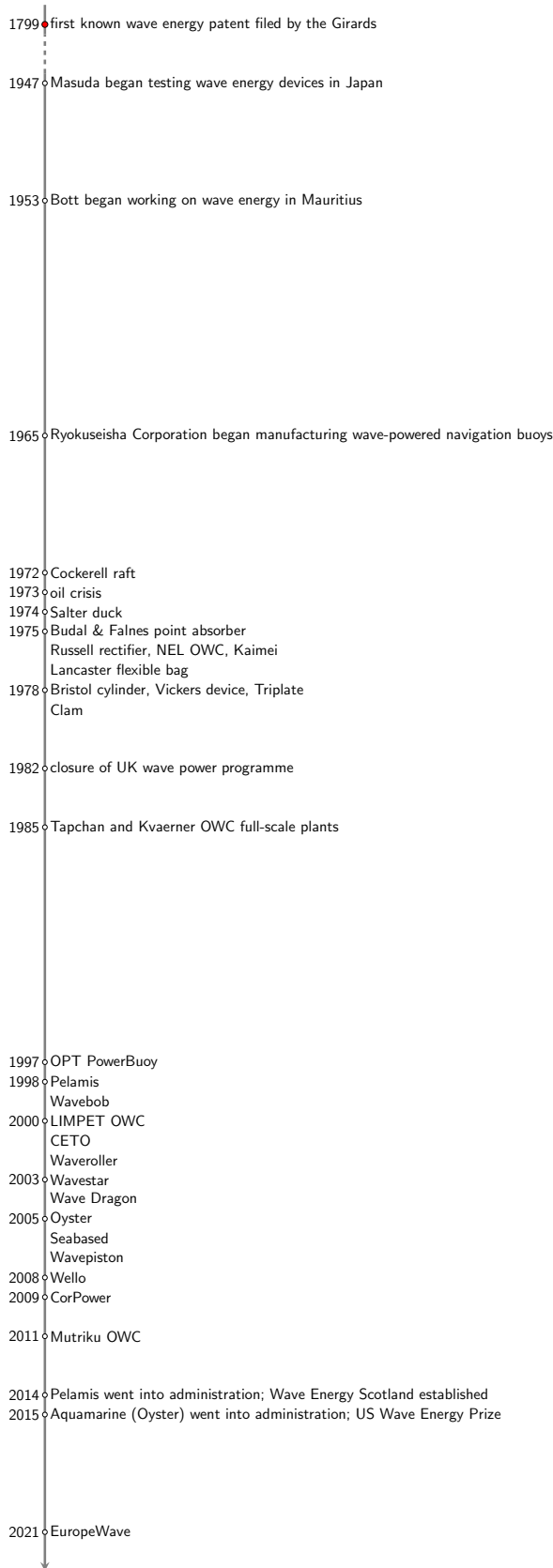


FIGURE 3: Wave energy timeline. Except for the period between 1799 and 1947, the length of the timeline is proportional to time.

3 A simple oscillator

Wave energy converters (WECs) come in a variety of forms. Although differing in forms, most of them are similar in principle. With the exception of overtopping devices, most WECs can be categorised as either *oscillating bodies* or *oscillating water columns*. The keyword here is oscillation. Oscillating bodies utilise motion relative to the sea bed or other bodies. Oscillating water columns utilise motion of water relative to a fixed or moving chamber (see Fig. 4). These motions are converted into useful form of energy by a power take-off (PTO) unit, which can either be a mechanical, hydraulic, pneumatic, or a direct drive system. The final product is usually electricity, although other uses are possible, such as desalination. Figs. 5–6 show some examples of oscillating-body and OWC devices that have been constructed in full scale.

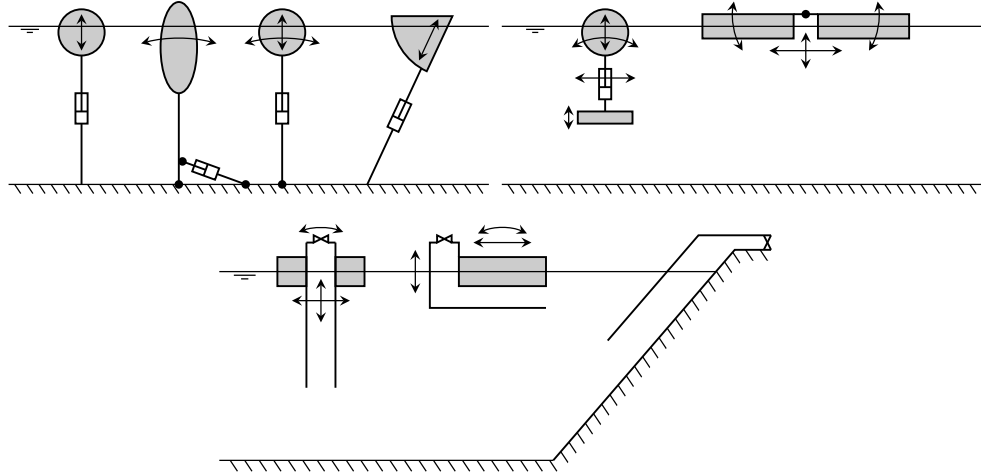


FIGURE 4: Oscillating bodies (top) and oscillating water columns (bottom). Arrows indicate modes of motion.

At its core, a WEC is an oscillator in water, driven by the waves. So, before considering how we can model a realistic WEC, let us first consider a simple oscillator, as shown in Fig. 7. Our aim is to understand the building blocks and the behaviour of a simple oscillator, which will be useful when it comes to understanding the behaviour of a WEC.

3.1 Equation of motion

The equation of motion of a simple oscillator with a constant mass m , as in Fig. 7, can be written, according to Newton's second law of motion, as

$$ma = m\ddot{x} = F + F_R + F_S, \quad (1)$$

where a is the acceleration, x is the displacement, F_R is the damping force, F_S is the spring force, and F is the excitation force. If the spring and damper have linear characteristics (which we will generally assume in these lectures), we can write

$$F_S = -Sx \quad \text{and} \quad F_R = -Ru = -R\dot{x}, \quad (2)$$

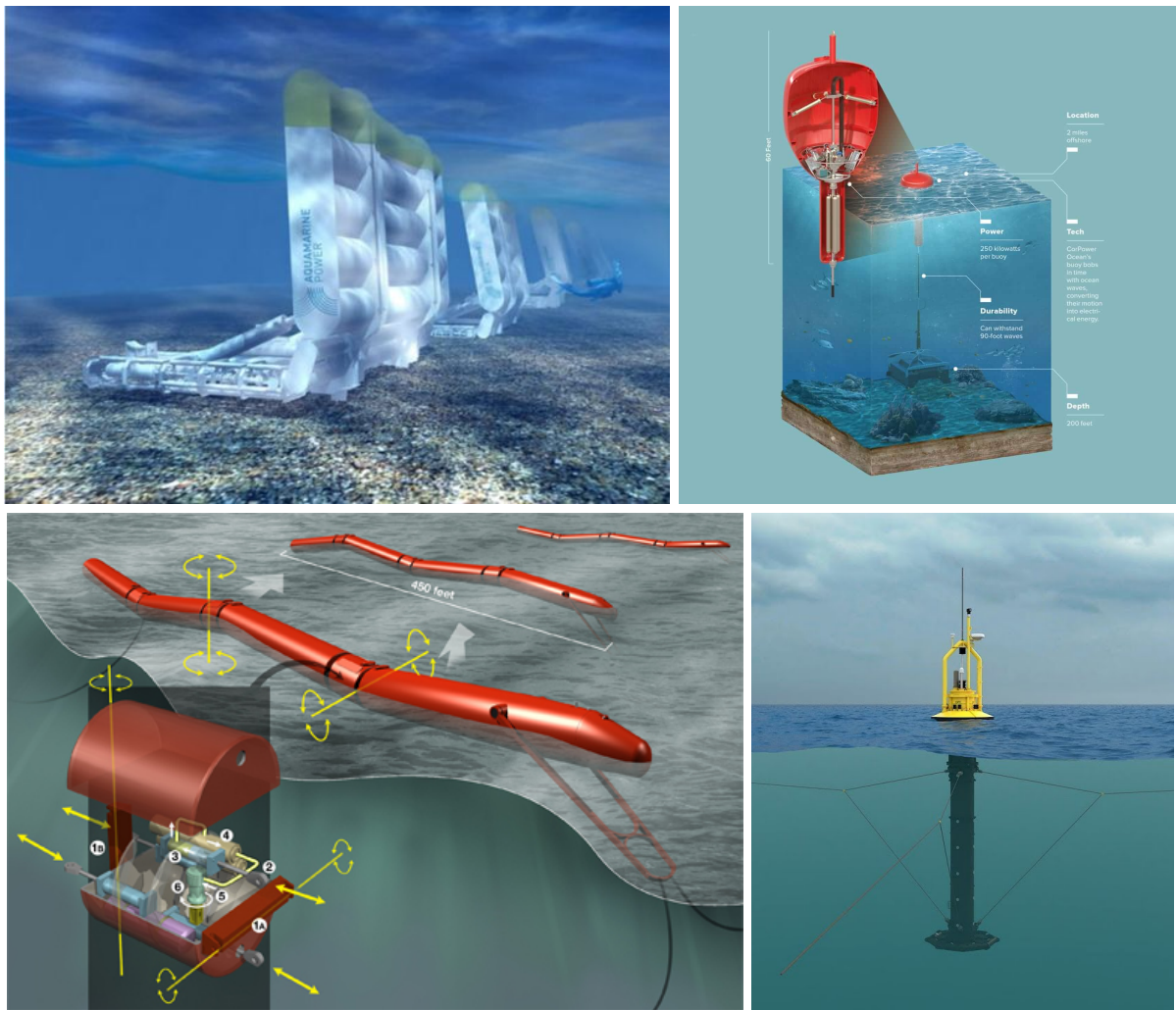


FIGURE 5: Examples of oscillating-body WECs. Clockwise from top left: Oyster, CorPower, OPT Power-Buoy, Pelamis.

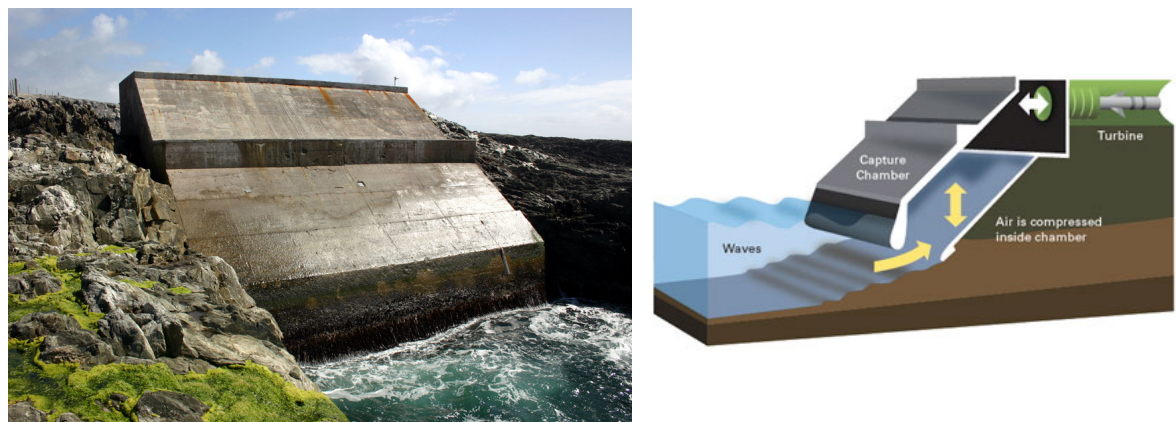


FIGURE 6: Example of oscillating-water-column WECs: Limpet OWC.

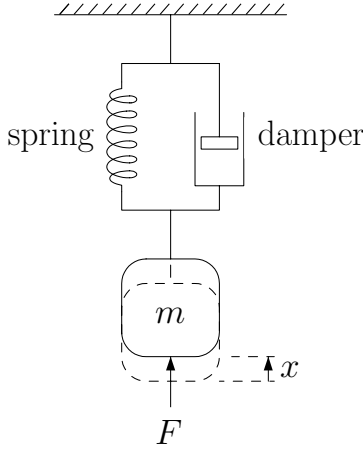


FIGURE 7: A simple oscillator, reproduced from [4].

where S and R are stiffness and damping coefficients. That is, the spring force is linearly proportional to the displacement, while the damping force is proportional to the velocity. Thus,

$$m\ddot{x} + R\dot{x} + Sx = F, \quad (3)$$

which is a second-order linear ordinary differential equation. We are mostly interested in cases where the excitation force F is a harmonic (sinusoidal) function of time, as in wave excitation.

3.2 Complex amplitudes

A useful tool for analysing harmonic oscillations is the notion of complex amplitudes.

With the use of Euler's formula

$$e^{i\psi} = \cos \psi + i \sin \psi, \quad (4)$$

or, equivalently,

$$\cos \psi = \operatorname{Re}\{e^{i\psi}\} = (e^{i\psi} + e^{-i\psi})/2, \quad (5)$$

$$\sin \psi = \operatorname{Im}\{e^{i\psi}\} = (e^{i\psi} - e^{-i\psi})/2i, \quad (6)$$

a harmonically oscillating quantity with frequency ω ,

$$x(t) = x_0 \cos(\omega t + \varphi_x), \quad (7)$$

where t is time, φ_x is the phase, and x_0 is the amplitude, can be written as

$$\begin{aligned} x(t) &= x_0 \operatorname{Re}\{e^{i(\omega t + \varphi_x)}\} \\ &= \operatorname{Re}\{x_0 e^{i\omega t} e^{i\varphi_x}\}. \end{aligned} \quad (8)$$

Introducing the complex amplitude

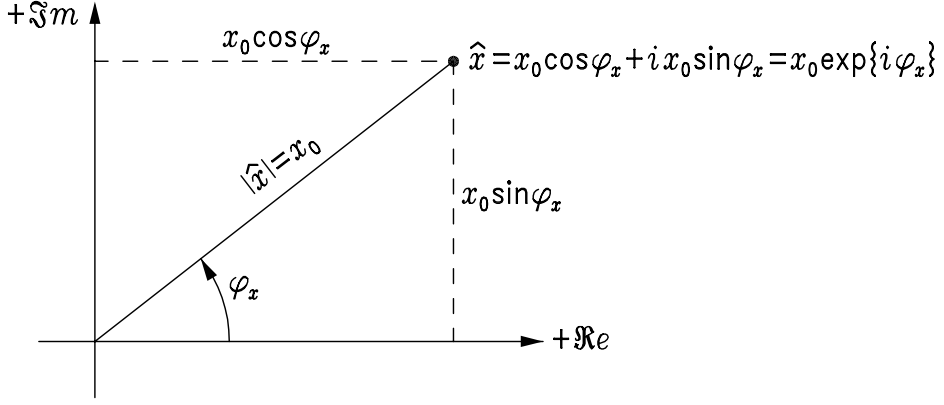


FIGURE 8: A complex amplitude \hat{x} contains information about the amplitude $x_0 = |\hat{x}|$ and the phase φ_x of the oscillating quantity $x(t)$. Reproduced from [4].

$$\hat{x} \equiv x_0 e^{i\varphi_x} \equiv |\hat{x}| e^{i\varphi_x}, \quad (9)$$

we can write (8) as

$$x(t) = x_0 \cos(\omega t + \varphi_x) = \operatorname{Re}\{\hat{x} e^{i\omega t}\}. \quad (10)$$

Furthermore, the first and second time derivative of $x(t)$ can be written as

$$u \equiv \dot{x} \equiv \frac{dx}{dt} = \operatorname{Re}\{i\omega \hat{x} e^{i\omega t}\}, \quad (11)$$

$$a \equiv \ddot{x} \equiv \frac{du}{dt} \equiv \frac{d^2x}{dt^2} = \operatorname{Re}\{-\omega^2 \hat{x} e^{i\omega t}\}. \quad (12)$$

Writing $u(t)$ in terms of the complex amplitude \hat{u} , and $a(t)$ in terms of the complex amplitude \hat{a} , we therefore have $\hat{u} = i\omega \hat{x}$ and $\hat{a} = i\omega \hat{u} = -\omega^2 \hat{x}$. Thus, to differentiate a harmonically oscillating quantity with respect to time is equivalent to multiplying its complex amplitude by $i\omega$.

The complex amplitude (9) can be represented as a vector in the complex plane (see Fig. 8). The amplitude $x_0 = |\hat{x}|$ is the modulus of the vector, while the phase φ_x is the angle between the vector and the real axis.

From

$$\hat{u} = i\omega \hat{x} \quad (13)$$

and making use of the identity $i = e^{i\pi/2}$, we also have

$$u_0 e^{i\varphi_u} = i\omega x_0 e^{i\varphi_x} = \omega x_0 e^{i(\varphi_x + \pi/2)}, \quad (14)$$

which gives

$$u_0 = \omega x_0 \quad \text{and} \quad \varphi_u = \varphi_x + \pi/2. \quad (15)$$

Similarly,

$$a_0 = \omega u_0 = \omega^2 x_0 \quad \text{and} \quad \varphi_a = \varphi_u + \pi/2 = \varphi_x + \pi. \quad (16)$$

From the phase relationships, we see that displacement lags velocity by $\pi/2$, whereas acceleration leads velocity by $\pi/2$.

3.3 Impedance and reactance

Returning to the simple oscillator, if the external force is harmonically varying with an angular frequency ω , i.e., if $F(t)$ is of the form

$$F(t) = F_0 \cos(\omega t + \varphi_F) = \operatorname{Re}\{F_0 e^{i\varphi_F} e^{i\omega t}\} = \operatorname{Re}\{\hat{F} e^{i\omega t}\}, \quad (17)$$

then the steady-state response (i.e. the response after the transients have decayed away) will also be harmonically varying and, if the system is linear, will vary with the same frequency ω , i.e., it will have the form

$$u(t) = u_0 \cos(\omega t + \varphi_u) = \operatorname{Re}\{u_0 e^{i\varphi_u} e^{i\omega t}\} = \operatorname{Re}\{\hat{u} e^{i\omega t}\}. \quad (18)$$

Substituting (17) and (18) into (3), we have

$$[i\omega m + R + S/(i\omega)]\hat{u} = \hat{F}, \quad (19)$$

after cancelling out the $e^{i\omega t}$ from both sides of the equation. Note that \hat{u} and \hat{F} are complex, whereas m , R , and S are real. This equation, which describes the simple harmonic motion of an oscillator, is the basic equation to describe the dynamics of many oscillating systems, including a wave energy converter.

We can write (19) more compactly as

$$Z\hat{u} = \hat{F}, \quad (20)$$

if we introduce the *impedance* Z , defined as

$$Z = R + i(\omega m - S/\omega) = R + iX, \quad (21)$$

where the imaginary part X of the impedance is called the *reactance*.

Note that m , R , and S are known parameters of the system. Thus, for a given \hat{F} , we can solve (20) for \hat{u} .

We can see from (21) that $X = 0$ when

$$\omega = \omega_0 = \sqrt{S/m}. \quad (22)$$

This is the *resonance* frequency. At this frequency, we have $Z = R$ and the velocity response amplitude, $|\hat{u}/\hat{F}|$, is maximum:

$$|\hat{u}/\hat{F}|_{\max} = (u_0/F_0)_{\max} = 1/|Z|_{\min} = 1/R. \quad (23)$$

3.4 Frequency response function

Looking at (19), we can observe that

- At the resonance frequency $\omega = \omega_0$, the reactance cancels ($X = 0$), and so $F = Ru$, i.e., the velocity is in phase with the external force (since R is real) and $u_0/F_0 = 1/R$.
- At $\omega \ll \omega_0$, the stiffness term dominates, i.e. $F \rightarrow Sx$, or the displacement is in phase with the external force (since S is real) and $u_0/F_0 = \omega/S$ (cf. (15)).
- At $\omega \gg \omega_0$, the inertial term dominates, i.e. $F \rightarrow ma$, or the acceleration is in phase with the external force (since m is real) and $u_0/F_0 = 1/\omega m$ (cf. (16)).

These explain why the (normalised) frequency response functions of the velocity amplitude and phase (relative to the phase of the external force) look like those in Fig. 9. At resonance, or $\omega\sqrt{m/S} = 1$, the velocity amplitude is maximum and in phase with the external force. At $\omega \ll \omega_0$, the slope of the curve in Fig. 9a is 1, because $|\hat{u}/\hat{F}| = \omega/S$, whereas at $\omega \gg \omega_0$, the slope of the curve is -1 , because $|\hat{u}/\hat{F}| = 1/\omega m$. At $\omega \ll \omega_0$, the displacement is in phase with the external force, and so the velocity leads the force by $\pi/2$. At $\omega \gg \omega_0$, the acceleration is in phase with the external force, and so the velocity lags the force by $\pi/2$.

As an exercise, try replotting Fig. 9 in linear scale instead of log scale!

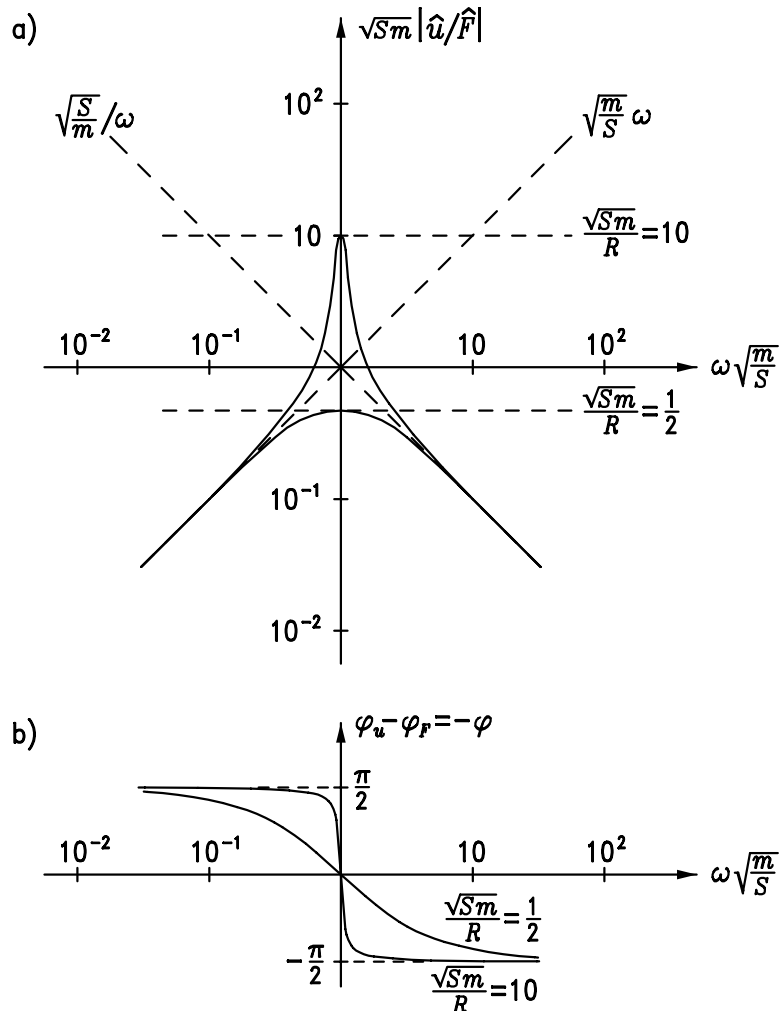


FIGURE 9: Frequency response functions of the (a) velocity amplitude and (b) phase, for two different damping coefficients R . Reproduced from [4].

3.5 Delivered power and consumed power

The *delivered* power is the power delivered by the external force into the system:

$$\begin{aligned}
P(t) &= F(t)u(t) = \operatorname{Re}\{\hat{F}e^{i\omega t}\}\operatorname{Re}\{\hat{u}e^{i\omega t}\} \\
&= \frac{1}{2}(\hat{F}e^{i\omega t} + \hat{F}^*e^{-i\omega t})\frac{1}{2}(\hat{u}e^{i\omega t} + \hat{u}^*e^{-i\omega t}) \\
&= \frac{1}{4}(\hat{F}\hat{u}^* + \hat{F}^*\hat{u} + \hat{F}\hat{u}e^{2i\omega t} + \hat{F}^*\hat{u}^*e^{-2i\omega t}) \\
&= \frac{1}{2}\operatorname{Re}\{\hat{F}\hat{u}^*\} + \frac{1}{2}\operatorname{Re}\{\hat{F}\hat{u}e^{2i\omega t}\}.
\end{aligned} \tag{24}$$

The second term is a harmonic oscillation with angular frequency 2ω and so has a zero time average. Hence, the time-average delivered power is

$$P \equiv \overline{P(t)} = \frac{1}{2}\operatorname{Re}\{\hat{F}\hat{u}^*\} = \frac{1}{2}\operatorname{Re}\{\hat{Z}\hat{u}\hat{u}^*\} = \frac{1}{2}\operatorname{Re}\{\hat{Z}|\hat{u}|^2\} = \frac{1}{2}R|\hat{u}|^2. \tag{25}$$

The *consumed* power is the power consumed by the damper:

$$\begin{aligned}
P_R(t) &= -F_R(t)u(t) = Ru^2(t) = R\operatorname{Re}\{\hat{u}e^{i\omega t}\}\operatorname{Re}\{\hat{u}e^{i\omega t}\} \\
&= \frac{1}{4}R(\hat{u}e^{i\omega t} + \hat{u}^*e^{-i\omega t})^2 \\
&= \frac{1}{4}R(2\hat{u}\hat{u}^* + \hat{u}^2e^{2i\omega t} + \hat{u}^{*2}e^{-2i\omega t}) \\
&= \frac{1}{2}R|\hat{u}|^2 + \frac{1}{2}\operatorname{Re}\{\hat{u}^2e^{2i\omega t}\}.
\end{aligned} \tag{26}$$

Again, the second term has a zero time average. Hence, the time-average consumed power is $\frac{1}{2}R|\hat{u}|^2$.

We see that the consumed power and the delivered power are equal in time average. This will be useful when we consider the (time-average) power absorbed by a WEC in section 6.2.

4 An oscillator in water

As a further step towards modelling a WEC, let us put our oscillator in water (see Fig. 10). This can be regarded as a simple WEC oscillating in a single mode (heave). Power is absorbed by the damper—this is our power take-off (PTO).

Let $F(t) = \operatorname{Re}\{\hat{F}e^{i\omega t}\}$. Assume a linear system. Thus, $u(t) = \operatorname{Re}\{\hat{u}e^{i\omega t}\}$. The (time-average) power consumed by the mechanical damper (our PTO) is

$$P_m = \frac{1}{2}R_m|\hat{u}|^2. \tag{27}$$

4.1 Radiation impedance

By analogy with (27), as the body oscillates in the water, it generates a wave which carries away *radiated power*

$$P_r = \frac{1}{2}R_r|\hat{u}|^2, \tag{28}$$

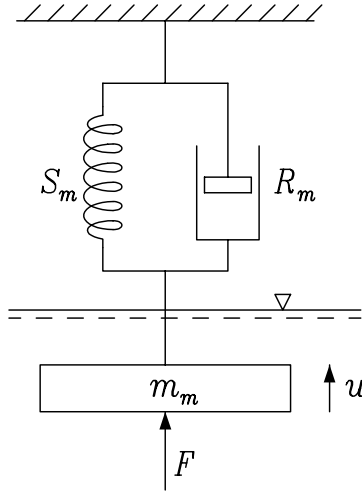


FIGURE 10: An oscillator in water, reproduced from [4].

which defines the radiation damping R_r . Due to the radiated wave, a force F_r acts on the body. Assuming a linear system, F_r is also harmonically varying, i.e.

$$F_r(t) = \text{Re}\{\hat{F}_r e^{i\omega t}\}. \quad (29)$$

Writing

$$\hat{F}_r = -Z_r \hat{u}, \quad (30)$$

we define the *radiation impedance* Z_r .

In general, Z_r is a complex function of frequency:

$$\begin{aligned} Z_r &= Z_r(\omega) = R_r(\omega) + iX_r(\omega) \\ &= R_r(\omega) + i\omega m_r(\omega), \end{aligned} \quad (31)$$

where R_r is the *radiation damping* and the radiation reactance X_r is conventionally written in terms of the *added mass* m_r . Note that in certain cases the added mass can be negative. The radiation impedance Z_r depends on the geometry of the radiating system. By geometry we mean the shape of the body and its mode of motion.

As an example, Fig. 11 shows the added mass and radiation damping of the geometry in Fig. 12. At $\omega \rightarrow 0$ or $\omega \rightarrow \infty$, an oscillating body generates no waves; so $R_r \rightarrow 0$ at these limits.

4.2 Wave excitation force

So far we have assumed the external force F to be a general external force that can be applied e.g. by a mechanical actuator. Let us now assume that the external force F is due to incident waves. In other words, let us consider a true WEC subjected to incident waves and absorbing energy from the waves.

Linear theory allows us to treat the problem of a body oscillating in response to incident waves, as a superposition of two sub-problems (see Fig. 13):

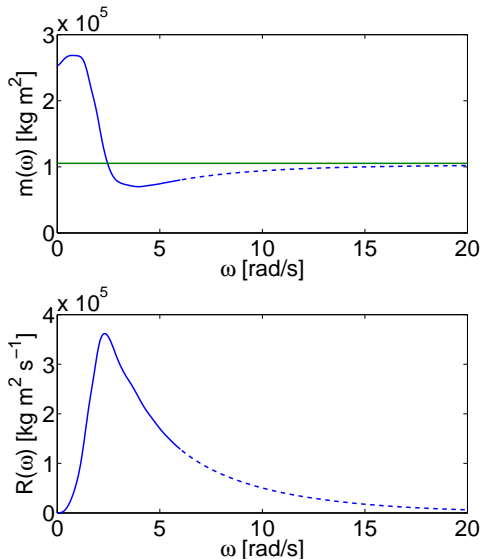


FIGURE 11: Added mass (top) and radiation damping (bottom) values calculated numerically using a boundary element method (BEM)-based code [13], reproduced from [8].

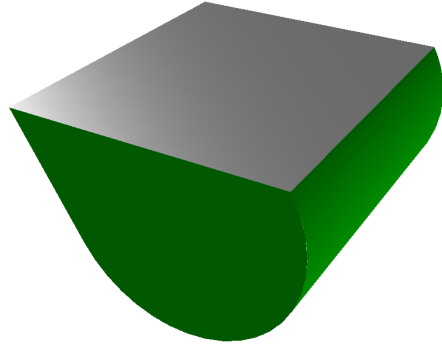


FIGURE 12: Geometry corresponding to the added mass and radiation damping in Fig. 11, reproduced from [8]. The geometry resembles the Salter Duck. It oscillates about a horizontal axis passing through the body. Only the shape below the water surface is shown.

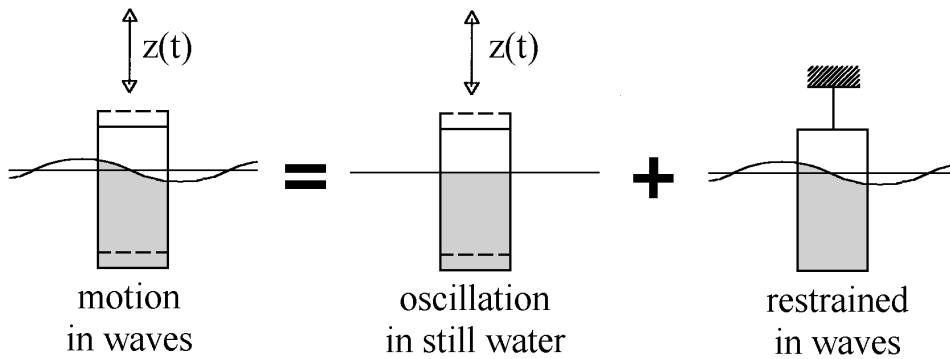


FIGURE 13: The problem of a body oscillating in response to incident waves is, according to linear theory, a superposition of radiation and diffraction problems. Reproduced from [7].

- *diffraction* problem

The body is fixed (not moving) and is subjected to incident waves.

- *radiation* problem

The body is oscillating with an unknown amplitude and phase, in otherwise still water (only waves radiated by the oscillating body are present).

The total hydrodynamic force F_t on the body is a superposition of the *wave excitation force* F_e and the *wave radiation force* F_r , where each is the force due to the wave acting on the body in each of the above problems:

$$F_t = F_e + F_r. \quad (32)$$

Note that F_r here is none other than the F_r discussed in the previous subsection.

Like F_r , the wave excitation force F_e is also a complex function of frequency. In linear theory,

F_e is proportional to the incident wave amplitude A :

$$\hat{F}_e(\omega) = \hat{f}_e(\omega)A, \quad (33)$$

where $\hat{f}_e(\omega)$ is defined as the excitation force coefficient. Note that A here is a complex amplitude.

4.3 Equation of motion

With incident wave, in reference to Fig. 10, we now have the following equation describing the motion of the oscillator:

$$[\mathrm{i}\omega m_m + R_m + S_m/(\mathrm{i}\omega)]\hat{u} = \hat{F}_e + \hat{F}_r, \quad (34)$$

which, upon substituting (30) and defining

$$Z_m \equiv \mathrm{i}\omega m_m + R_m + S_m/(\mathrm{i}\omega), \quad (35)$$

becomes

$$\begin{aligned} Z_m \hat{u} &= \hat{F}_e - Z_r \hat{u} \\ (Z_m + Z_r) \hat{u} &= \hat{F}_e. \end{aligned} \quad (36)$$

In this form, we have rearranged the terms such that only the excitation force appears on the right-hand side. We have defined two impedances: the mechanical impedance Z_m and the radiation impedance Z_r .

We can solve this equation for the velocity:

$$\begin{aligned} \hat{u} &= \frac{\hat{F}_e}{Z_m + Z_r} \\ &= \frac{\hat{F}_e}{R_m + R_r + \mathrm{i}[\omega(m_m + m_r) - S_m/\omega]}, \end{aligned} \quad (37)$$

where the last equality follows from (35) and (31).

5 Absorbed power

Knowing the velocity \hat{u} , we can calculate the absorbed power. The time-average power absorbed in the mechanical damper is

$$P_a = \frac{R_m}{2} |\hat{u}|^2 = \frac{(R_m/2) |\hat{F}_e|^2}{(R_m + R_r)^2 + [\omega(m_m + m_r) - S_m/\omega]^2}. \quad (38)$$

Observe that $P_a = 0$ for $R_m = 0$ (no PTO damping). Also, $P_a = 0$ for $R_m = \infty$ (infinite PTO damping). Somewhere in between, the absorbed power is maximum. To find the value of R_m that maximises the absorbed power, we solve $\frac{\partial P_a}{\partial R_m} = 0$, which gives

$$R_{m,\text{opt}} = \sqrt{R_r^2 + X^2}, \quad (39)$$

$$P_{a,\text{max}} = \frac{|\hat{F}_e|^2}{4(R_r + R_{m,\text{opt}})}. \quad (40)$$

Here,

$$X = \omega(m_m + m_r) - S_m/\omega \quad (41)$$

is the total reactance. The proof for the above results, (39) and (40), is left as an exercise.

Equation (39) is called the *optimum amplitude condition*, since it specifies how much damping is required to give the optimum motion amplitude that will maximise the absorbed power at any given frequency (when the phase is not necessarily optimum).

If $X = 0$ (resonance), then the absorbed power is maximum when

$$R_{m,\text{OPT}} = R_r, \quad (42)$$

which is obtained by setting $X = 0$ in (39). This gives

$$P_{a,\text{MAX}} = \frac{|\hat{F}_e|^2}{8R_r}, \quad (43)$$

which is obtained by substituting (42) into (40). The optimum velocity is obtained by substituting $X = 0$ and $R_{m,\text{OPT}} = R_r$ into (37), which gives

$$\hat{u}_{\text{OPT}} = \frac{\hat{F}_e}{2R_r}. \quad (44)$$

We call $X = 0$ the *optimum phase condition*. When the body oscillates with the velocity as given by (44), it satisfies both the optimum amplitude and the optimum phase conditions. $P_{a,\text{MAX}}$ as given by (43) is the ultimate maximum absorbed power than can possibly be absorbed by the oscillator from the waves (provided it can realise the optimum motion as given by (44)). $P_{a,\text{max}}$ as given by (40) is less than or equal to $P_{a,\text{MAX}}$.

Observe from (43) that $P_{a,\text{MAX}}$ is purely a function of the wave excitation force \hat{F}_e and the radiation damping R_r . In other words, the maximum possible power that can be absorbed from the wave is governed by the hydrodynamic properties of the body, not by the power take-off system. Since \hat{F}_e and R_r depend on the geometry of the system (body size, shape, and mode of motion), $P_{a,\text{MAX}}$ also depends on the geometry of the system. Note that since \hat{F}_e and R_r vary with frequency, the maximum absorbed power $P_{a,\text{MAX}}$ and the required optimum motion \hat{u}_{OPT} also vary with frequency. This highlights the importance of bandwidth, since real ocean waves consist of multiple frequency components.

As an example, Fig. 14 shows the absorbed power of two oscillators as a function of frequency, for an incident wave amplitude of 0.5 m. The two oscillators are made of the same body, i.e. a circular cylinder, but oriented differently and oscillating in different modes. The one at the top is

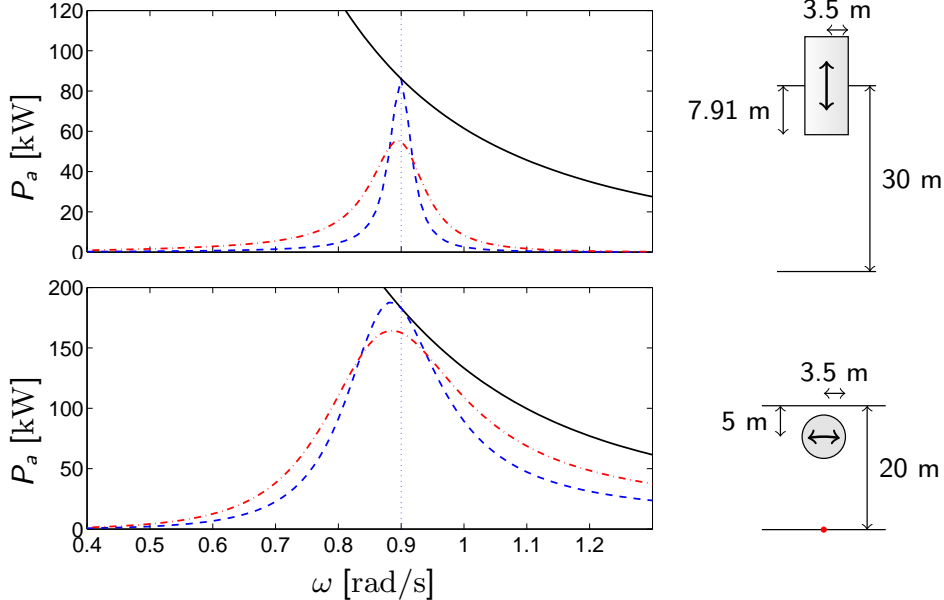


FIGURE 14: Power absorption characteristics of two oscillators. Solid line: maximum absorbed power $P_{a,\text{MAX}}$; dashed and dash-dotted lines: absorbed power P_a for different mechanical damping R_m values. The blue dashed lines are obtained with $R_m = R_r(\omega_0)$, whereas the red dash-dotted lines are obtained with $R_m > R_r(\omega_0)$. Adapted from [10].

oriented vertically and is oscillating in heave (vertical direction). The one at the bottom is oriented horizontally and is oscillating about a hinge at the seabed. However, the two oscillators are tuned to have the same resonance frequency $\omega_0 = 0.9 \text{ rad/s}$. In each plot there are three lines: the solid black line is the maximum absorbed power $P_{a,\text{MAX}}$ as given by (43); the dashed blue line and the dash-dotted red line are both the absorbed power P_a as obtained from (38) with constant R_m , but the dashed blue line is obtained with $R_m = R_r(\omega_0)$, whereas the dash-dotted red line is obtained with R_m that is greater than $R_r(\omega_0)$.

Observe how the absorbed power P_a varies with frequency ω , and how $P_a = P_{a,\text{MAX}}$ when both $X = 0$ and $R_m = R_r$ (as shown by the blue dashed lines touching the black solid lines at $\omega = \omega_0 = 0.9 \text{ rad/s}$). If either of these conditions is not met, then $P_a(\omega) < P_{a,\text{MAX}}(\omega)$, as when $\omega \neq \omega_0$ (the blue dashed lines are no longer touching the black solid lines away from ω_0) or when $R_m > R_r$ (the red dash-dotted lines are never touching the black solid lines). The bandwidth of the absorbed power P_a (the broadness of the curve) depends on hydrodynamic (in turn, on geometry) as well as mechanical properties of the system. Increasing the mechanical damping R_m reduces the peak of the curve but broadens the bandwidth.

In reality, P_a is also limited by losses and practical constraints, which we will discuss later.

5.1 Capture width (absorption width)

The power performance of a WEC is normally expressed in terms of its *capture width*, defined as the ratio between the absorbed power and the wave-power level:

$$d_a \equiv \frac{P_a}{J}. \quad (45)$$

This can be understood as the width of the wave front carrying the same amount of energy as that absorbed by the WEC. The capture width can be expressed in terms of the incident wavelength λ , as we will show later. For some simple geometries, there exists simple expressions for the maximum capture width, e.g.

$$d_{a,\text{MAX}} = \frac{\lambda}{2\pi} \text{ for a heaving axisymmetric body.} \quad (46)$$

Example A WEC in the form of a vertical circular cylinder is absorbing wave energy through its vertical motion. What is its maximum capture width in regular wave of period 8 s and amplitude 1 m? Theoretically, how much power can it potentially absorb from this wave? Assume deep water condition.

Answer The expression for a heaving axisymmetric body, $d_{a,\text{MAX}} = \frac{\lambda}{2\pi}$, applies. The wavelength for $T = 8$ s, assuming deep water condition, is (from deep-water dispersion equation)

$$\lambda = \frac{gT^2}{2\pi} = \frac{9.81 \times 8^2}{2\pi} \approx 100 \text{ m.} \quad (47)$$

Thus, $d_{a,\text{MAX}} = \frac{\lambda}{2\pi} \approx \frac{100}{2\pi} \approx 16 \text{ m.}$ The wave-power level available in the (deep-water) regular waves is approximately $J \approx TH^2 = 8 \times 2^2 = 32 \text{ kW/m.}$ The maximum power that it can potentially absorb is therefore

$$P_{a,\text{MAX}} = d_{a,\text{MAX}} J \approx 16 \times 32 \approx 500 \text{ kW.} \quad (48)$$

5.2 Capture width ratio

Dividing the capture width by the frontal width of the WEC, we get a nondimensional quantity often referred to as the *capture width ratio*:

$$\text{CWR} = \frac{d_a}{D}, \quad (49)$$

where D is the width of the WEC. Some people call this quantity ‘efficiency’, but note that its value can be greater than unity, making it inappropriate to call it efficiency.

6 Principles of wave energy absorption

6.1 Wave absorption as destructive interference

One key principle of wave energy absorption (by oscillating systems) is that *to absorb a wave is to generate a wave*.

To illustrate this, consider a wave flume terminating with a rigid wall at the end, as in Fig. 15. The incident wave propagates from left to right. The incoming energy is proportional to the square of the incident wave amplitude. If the wall is completely rigid, the wave will be totally reflected,

so the reflected wave amplitude is equal to the incident wave amplitude. The outgoing energy is therefore equal to the incoming energy. The energy absorbed by the wall, which is given by the difference between the incoming energy and the outgoing energy, is zero in this case.

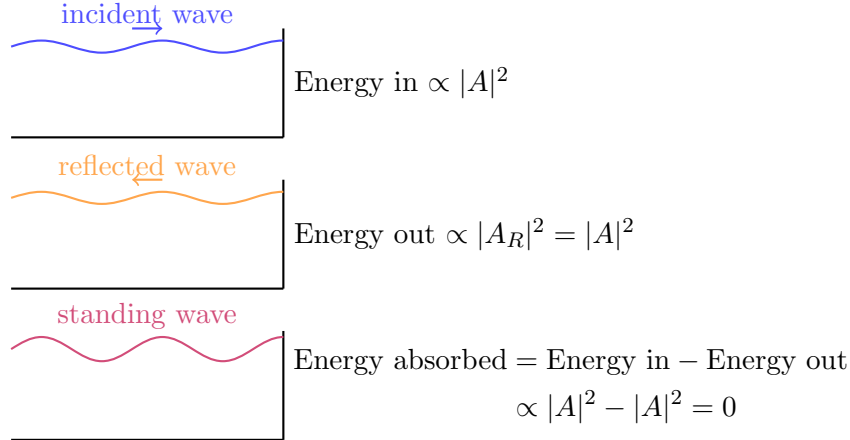


FIGURE 15: Incident wave reflected by a rigid wall, resulting in a standing wave.

Let us now allow the wall to oscillate about a hinge at the bottom, as in Fig. 16. Again, the incident wave will be diffracted by the wall, but in this case, the oscillation of the wall radiates a wave that also propagates to the left. If the wall is made to oscillate in such a way that the radiated wave cancels out the diffracted wave, then the outgoing energy is zero. The energy absorbed by the wall is therefore equal to the incoming energy. In other words, the incident wave energy is completely absorbed by the wall. This is possible only because the wall is generating a wave.

The oscillating wall becomes a perfect wave absorber provided it can generate a wave of the right amplitude and phase to cancel out the incident wave. This illustrates the optimum amplitude and optimum phase conditions for maximum power absorption, which we discussed in section 5.

Moving on to a more realistic case, let us consider a WEC in a flume, where there is water to the left as well as to the right of the WEC, as in Fig. 17. In this case, we need to take into account both sides of the WEC. The incident wave again propagates from left to right. The incoming energy from the left is proportional to the square of the incident wave amplitude. The incoming

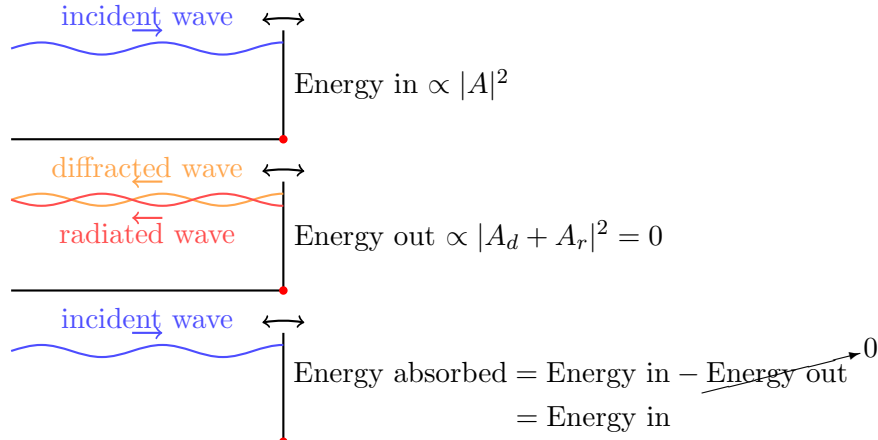


FIGURE 16: The incident wave is completely absorbed if the wall generates radiated wave that cancels out the diffracted wave. This requires the phase and amplitude to be optimal.

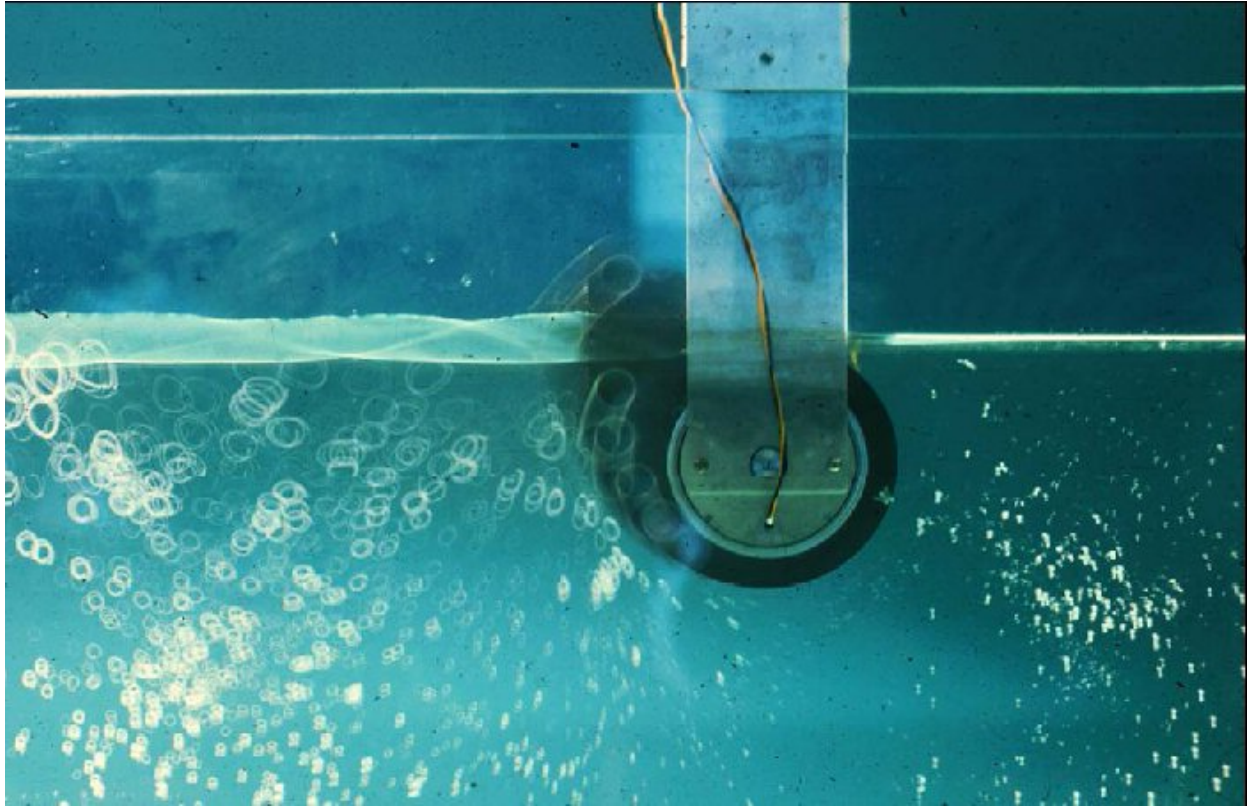


FIGURE 17: Salter Duck in a wave flume. Incident waves propagate from left to right. Reproduced from [12].

energy from the right is zero, since there is no wave coming from the right. The outgoing wave from the WEC to the left is the sum of the diffracted wave and radiated wave going to the left, $A_d^- + A_r^-$. The outgoing wave from the WEC to the right is the sum of the diffracted and radiated waves going to the right plus the incident wave, $A_d^+ + A_r^+ + A$. The absorbed energy is therefore proportional to $|A|^2 - |A_d^- + A_r^-|^2 - |A + A_d^+ + A_r^+|^2$. From here it is clear that since the second and third terms are always positive, perfect absorption is only possible if the WEC radiates waves that cancel out the diffracted wave going to the left and the sum of the incident and diffracted waves going to the right.

Example Fig. 17 shows a 1-second exposure photograph (taken in 1976) of a scaled model of the Salter Duck in a wave flume. Estimate the proportion of the incident wave energy being absorbed by the Duck.

Answer The thick band on the left indicates that $|A_d^- + A_r^-| \ll |A|$ (waves going to the left is much smaller than the incident wave). This we can tell by observing the depth of the kinks in the band (which gives the height of the outgoing wave to the left) relative to the average thickness of the band (which gives the height of the incident wave). This appears to be about 1/5. In addition, the thin band on the right indicates that $|A + A_d^+ + A_r^+| \approx 0$ (waves going to the right is almost zero). Since wave energy is proportional to the height (or amplitude) squared, this means that 1/25 or 4% of the incoming energy is going to the left and, therefore, $100\% - 4\% - 0\% = 96\%$ of the incoming energy is being absorbed by the Duck.

For a WEC in the open sea, the principle stands. Absorbing wave energy means that energy has to be removed from the waves. Hence, there must be a cancellation or reduction of waves which pass a WEC or are reflected from it. Such cancellation or reduction of waves can be realised by the oscillating WEC, provided it generates waves which oppose (are in counterphase with) the passing and/or reflected waves. The task of a WEC is to generate a wave that interferes destructively with the other waves such that if we define a control volume enclosing the WEC, the energy that goes out of the volume is less than the energy that goes into the volume. To maximise this cancellation, the phase and amplitude of oscillation of the WEC have to be optimum.

6.2 Absorbed power

The key principle that we have illustrated above, that it is necessary for a WEC to radiate a wave in order to absorb a wave, can be proven mathematically. Consider again a single oscillator (a WEC oscillating in one mode) subjected to incident wave (cf. section 4.3):

$$\begin{aligned} [\mathrm{i}\omega m_m + R_m + S_m/(\mathrm{i}\omega)]\hat{u} &= \hat{F}_e + \hat{F}_r \\ (R_m + \mathrm{i}X_m)\hat{u} &= \hat{F}_e - Z_r\hat{u} \end{aligned} \quad (50)$$

Multiplying each term by $\hat{u}^*/2$ and taking the real part, we obtain the time-average power (cf. section 3.5):

$$\begin{aligned} \mathrm{Re}\{(R_m + \mathrm{i}X_m)\hat{u}\hat{u}^*/2\} &= \mathrm{Re}\{(\hat{F}_e - Z_r\hat{u})\hat{u}^*/2\} \\ \underbrace{\frac{R_m}{2}|\hat{u}|^2}_{P_a} &= \underbrace{\frac{1}{2}\mathrm{Re}\{\hat{F}_e\hat{u}^*\}}_{P_e} - \underbrace{\frac{R_r}{2}|\hat{u}|^2}_{P_r}. \end{aligned} \quad (51)$$

We can see that the absorbed power P_a is equal to the excitation power P_e minus the radiated power P_r . In other words, the absorbed power can be obtained without knowing the details of the power take-off system. (Remember from section 3.5 that the delivered power and the consumed power are equal in time average.)

The excitation power can be written as

$$\begin{aligned} P_e &= \frac{1}{2}\mathrm{Re}\{\hat{F}_e\hat{u}^*\} \\ &= \frac{1}{2}\mathrm{Re}\{|\hat{F}_e|e^{\mathrm{i}\varphi_e}|\hat{u}|e^{-\mathrm{i}\varphi_u}\} \\ &= \frac{1}{2}|\hat{F}_e||\hat{u}|\cos\gamma, \end{aligned} \quad (52)$$

where $\gamma = \varphi_u - \varphi_F$, the phase difference between u and F_e . (Note that, when the total reactance $X = 0$ (cf. (41)), we have $\gamma = 0$ and hence $\cos\gamma = 1$ and $P_e = \frac{1}{2}|\hat{F}_e||\hat{u}|$.)

From (51)–(52) we see that P_e is *linear* in $|\hat{u}|$, while P_r is *quadratic* in $|\hat{u}|$. Plotting P_e and P_r against $|\hat{u}|$, we have the plot in Fig. 18.

Solving $\frac{\partial P_a}{\partial |\hat{u}|} = 0$ or inspecting the plot, we find that the absorbed power $P_a = P_e - P_r$ is maximised when

$$P_{a,\max} = P_{r,\text{opt}} = \frac{1}{2}P_{e,\text{opt}}. \quad (53)$$

In other words, for maximum power absorption, the WEC has to radiate as much power as it absorbs. Thus, we have shown that it is *necessary* for the WEC to radiate waves in order to absorb any power from the waves. If the WEC does not radiate any waves (such as when it is held fixed), then the absorbed power will be zero. Likewise, if the radiated waves are too large, then the absorbed power will be zero or even negative (power is input into rather than taken out of the waves). Equation (53) is true for any oscillating WEC system, including arrays of multiple WECs. In the latter case, the total maximum absorbed power is equal to the total radiated power.

The optimum velocity amplitude (obtained by solving $\frac{\partial P_a}{\partial |\hat{u}|} = 0$) is

$$|\hat{u}_{\text{opt}}| = \frac{|\hat{F}_e|}{2R_r} \cos \gamma. \quad (54)$$

If, in addition, u is in phase with F_e , i.e. $\gamma = 0$, then

$$\hat{u} = \hat{u}_{\text{OPT}} = \frac{\hat{F}_e}{2R_r}, \quad (55)$$

which gives

$$P_a = P_{a,\text{MAX}} = \frac{|\hat{F}_e|^2}{8R_r}. \quad (56)$$

Observe that these are the same results as we have seen before, when we solved for the optimum damping R_m (see (43) and (44)).

Thus, we have shown two routes to the same set of results, one by optimising the power take-off damping R_m , and the other by optimising the body velocity $|\hat{u}|$ without caring about the detail of the power take-off.

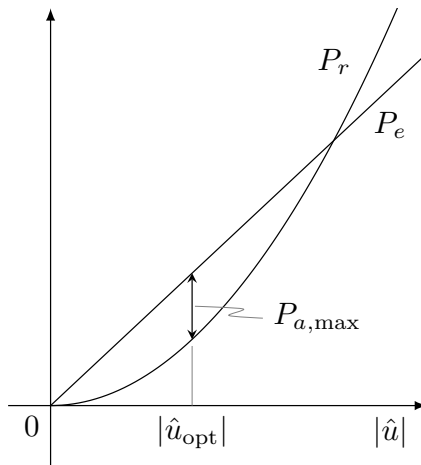


FIGURE 18: The variation of the excitation power P_e and the radiated power P_r with the body velocity $|\hat{u}|$.

6.3 Far-field theory

There is yet another route to the same result, which is by considering only the far field, without caring about the detail of the WEC. If we imagine a vertical cylinder enclosing all WECs in the system, with a large diameter such that the cylinder wall is sufficiently far from the WECs, such as in Fig. 19, then the absorbed power is the net wave power that is transported into the

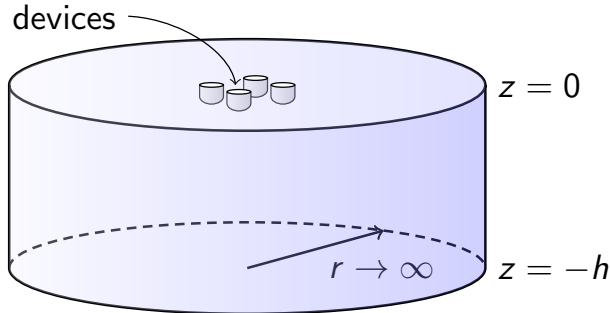


FIGURE 19: An envisaged cylinder containing the WEC system.

cylinder. Recalling the definition of intensity from Part 1, we find that the absorbed power is the intensity integrated over the surface area of the cylinder:

$$P_a = - \int_{-h}^0 \int_0^{2\pi} \underbrace{\frac{1}{2} \text{Re}\{pv_r^*\}}_{\text{intensity}} r d\theta dz, \quad (57)$$

where p is the total hydrodynamic pressure and v_r is the r -component of the total fluid velocity. The negative sign is because r is pointing outward, whereas we are interested in the net power *into* the cylinder. The integral is taken only over the vertical surface of the cylinder since there is no energy transport through the horizontal surfaces (the sea bed and the free surface). Each of p and v_r is a sum of three terms associated with the incident, diffracted, and radiated waves. Without going into the details, the maximum mean absorbed power can be shown to be

$$P_{a,\text{MAX}} = \frac{J}{k} G, \quad (58)$$

where J is the wave-power level, $k = 2\pi/\lambda$ is the wavenumber, and G is the optimum gain function. The optimum gain function G is related to the far-field pattern of waves radiated by the WEC system when it oscillates optimally. The general expression for G is rather complicated, but it shows that a system capable of radiating waves in one predominant direction has a high $P_{a,\text{MAX}}$.

Simple expressions for the optimum gain function exist for simple geometries. For a monopole radiator, i.e., a body making a wave radiation pattern as in Fig. 20 (left), e.g. an axisymmetric body oscillating in heave,

$$G = 1, \quad (59)$$

$$d_{a,\text{MAX}} = \frac{1}{k} = \frac{\lambda}{2\pi}. \quad (60)$$

FIGURE 20: Wave radiation pattern from a monopole (left) and from a dipole (right). Animation courtesy of Dr. Dan Russell, Grad. Prog. Acoustics, Penn State.

For a dipole radiator, i.e., a body making a wave radiation pattern as in Fig. 20 (right), e.g. a small body oscillating in surge or pitch,

$$G = 2, \quad (61)$$

$$d_{a,\text{MAX}} = \frac{2}{k} = \frac{\lambda}{\pi}. \quad (62)$$

In summary, the key principles of wave energy absorption are as follows:

- It is impossible to absorb a wave without radiating a wave (with the exception of overtopping devices).
- Our aim is not to make the WEC respond as much as possible, but respond at the right phase and amplitude. Not only the amplitude but also the phase of the oscillation have to be optimal (easy for regular wave, but challenging for irregular wave).
- A good wave absorber or an array of wave absorbers needs to be good at making waves (into one predominant direction). Note that a good wave absorber is not necessarily a good WEC, because a good WEC will not only need to have a good wave absorption but also need to be able to do this at minimum cost.
- It is important to have as broad resonance bandwidth as possible. More on this in the next subsection.

6.4 Resonance bandwidth

We have earlier touched upon resonance bandwidth. Because a real sea is composed of many frequency components, it is important for a WEC to have as broad resonance bandwidth as possible. The resonance bandwidth $\Delta\omega$ is defined as the frequency interval $\omega_u - \omega_l$ in which the relative absorbed-power response $\frac{P_a(\omega)/|\hat{F}_e(\omega)|^2}{P_a(\omega_0)/|\hat{F}_e(\omega_0)|^2}$ exceeds $\frac{1}{2}$. Here, ω_0 is the resonance frequency of the system. The relative bandwidth is defined as $\frac{\Delta\omega}{\omega_0}$ and can be shown to be given by (see Assignment)

$$\frac{\Delta\omega}{\omega_0} = \frac{\text{damping}}{\sqrt{\text{stiffness} \times \text{mass}}}. \quad (63)$$

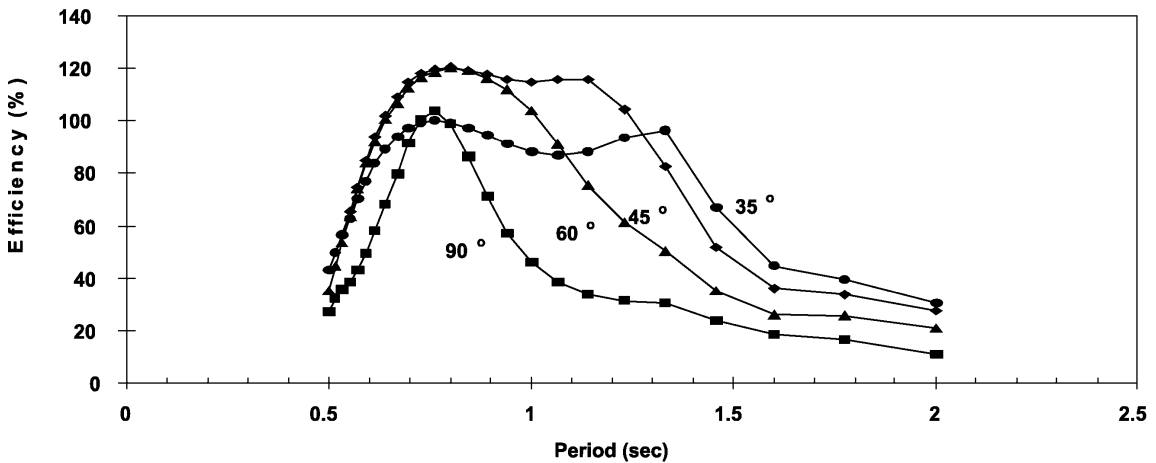
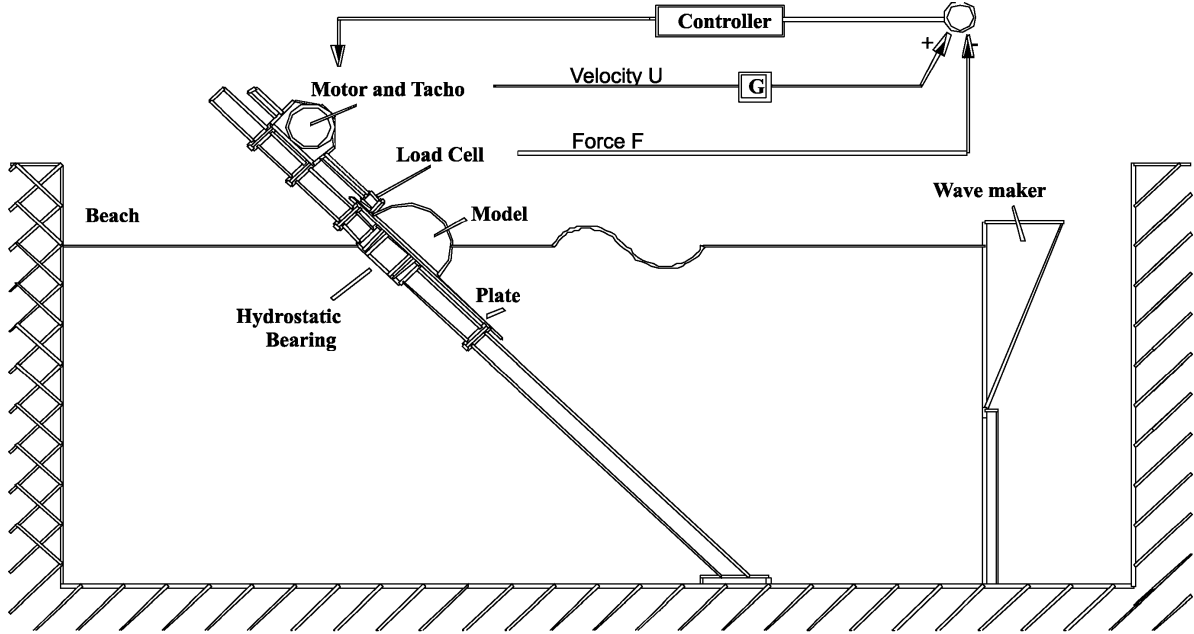


FIGURE 21: Example of how resonance bandwidth is dependent on geometry (the slope of the incline along which the body is oscillating). Vertical motion corresponds to 90° . Reproduced from [12].

Remember that the resonance period T_0 is given as (cf. (22))

$$T_0 = 2\pi \sqrt{\frac{\text{mass}}{\text{stiffness}}} \quad (64)$$

and that for a WEC oscillating in a single mode, the optimum phase for maximum power absorption happens at resonance. Therefore, in terms of the economics of the WEC, we want T_0 to be as large as possible relative to the device size. To do this, according to (64) we can either increase its mass or decrease its stiffness. However, as seen from (63), increasing the mass also reduces the bandwidth, whereas decreasing the stiffness broadens the bandwidth. This means that it is generally a better strategy to decrease the stiffness of the device than to increase its mass.

Geometry (shape and mode of motion) plays an important role, since it influences all three parameters (damping, stiffness, and mass) at the same time. We have looked at this briefly in

the example given in Fig. 14. Fig. 21 is another example. Here we have a WEC in the form of a body oscillating along an incline. The bottom plot shows the measured capture width ratio of the device. Changing the slope of the incline changes the power absorption characteristics of the device. Having the incline at 45° to horizontal is seen to be optimal. The broadening of the bandwidth arises from a combination of both a reduction in hydrostatic stiffness and a variation in the radiation damping and added mass of the body as the inclination angle is decreased.

6.5 Budal's upper bound

Before concluding this section, let us consider the limitation to the absorbed power arising from physical constraints of the device. For example, if the body is connected to a piston for power take off, this piston may have a stroke limit. It is then impossible for the body to move beyond this limit. However, the optimum velocity (or displacement) that is required for maximum power absorption may exceed this physical constraint. In this case, it is no longer possible to achieve the theoretical maximum absorbed power. There is an upper bound to the absorbed power associated with the finite displacement stroke of the device.

Recall from (51) and (52) that the absorbed power can be written as

$$\begin{aligned} P_a &= P_e - P_r \\ &= \frac{1}{2} |\hat{F}_e| |\hat{u}| \cos \gamma - \frac{1}{2} R_r |\hat{u}|^2. \end{aligned} \quad (65)$$

Since $\cos \gamma \leq 1$ and the radiated power $P_r = \frac{1}{2} R_r |\hat{u}|^2$ cannot be negative, we have

$$P_a < \frac{1}{2} |\hat{F}_e| |\hat{u}|. \quad (66)$$

Due to the displacement limit, the displacement amplitude cannot be greater than $|\hat{s}_{\max}|$, which means

$$|\hat{u}| < \omega |\hat{s}_{\max}|. \quad (67)$$

For a heaving body, it is known that

$$|\hat{F}_e| < \rho g S_w |A|, \quad (68)$$

where S_w is the waterplane area. If the body is cylindrical with a vertical axis of symmetry, then the maximum displacement limit can be written as

$$|\hat{s}_{\max}| = V / (2S_w), \quad (69)$$

where V is the volume stroke (see Fig. 22). Therefore,

$$P_a < \frac{\rho g \omega |A|}{4} V = \frac{\pi \rho g H}{4T} V. \quad (70)$$

This result was first derived by Budal.

Therefore, there are two upper bounds to the absorbed power of a WEC. The first, P_A , is the upper bound due to optimal wave interference, assuming the WEC can realise the required

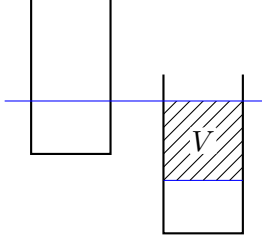


FIGURE 22: The volume stroke of a cylindrical body is equal to the waterplane area times the maximum displacement stroke. The displacement stroke is equal to two times the displacement amplitude.

optimum motion. In general (cf. 58),

$$P_a < P_A = \frac{J}{k}G, \quad (71)$$

where G is the optimum gain function, specific for the WEC or the WEC array. For an axisymmetric heaving WEC in deep water,

$$P_a < P_A = P_{a,\text{MAX}} = \frac{\lambda}{2\pi}J = \frac{\rho g^3 T^3 H^2}{128\pi^3}, \quad (72)$$

where we have used the exact expression of J and λ for deep-water regular wave (see equations (12)–(13) of Part 1).

The second, P_B (the Budal upper bound), is the upper bound due to the physical constraint of the WEC (the WEC has a finite volume stroke; it can displace only a finite volume of water, which may be less than what is required for optimal wave interference). In general,

$$P_a < P_B \propto \frac{H}{T}. \quad (73)$$

For a vertical cylindrical WEC moving in heave,

$$P_a < P_B = \frac{\rho g \omega |A|}{4}V = \frac{\pi \rho g H}{4T}V. \quad (74)$$

The two upper bounds, P_A and P_B , are plotted in Fig. 23 for a heaving vertical circular cylinder. Because of the physical limitations of the device (a finite stroke length), the theoretical maximum for $T \gtrsim 8$ s is not realisable.

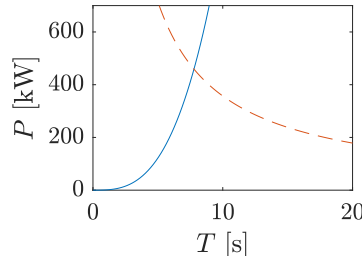


FIGURE 23: Two upper bounds to the power absorbed by a heaving vertical circular cylinder of volume stroke $V = 226 \text{ m}^3$. Solid line is P_A , dashed line is P_B .

7 Physical modelling

Before building an actual WEC in full scale, a WEC developer must have a high level of understanding of how the WEC would respond in a given environmental (wave) condition. Both physical and numerical modelling are critical to provide this understanding. We discuss physical modelling in this section and numerical modelling in the next.

There are a number of reasons for conducting physical model tests: to prove a concept, to validate numerical predictions or theory, or to better understand physical problems not predictable otherwise.

What is a physical model? It is a physical system reproduced at a reduced size so that the dominant forces are represented in the model in correct proportion to the prototype. To ensure similitude between prototype and model, the following requirements must be met: *geometric similarity* (ratio between geometrical dimensions), *kinematic similarity* (ratio between motions), *dynamic similarity* (ratio between forces). It is impossible to satisfy all of these for *all* forces, but they must be satisfied for the dominating physics. Violations are called *scale effects*. For WECs, scale effects could arise from air compressibility (relevant for WECs utilising air flow, e.g. oscillating water columns and flexible bag devices), viscosity, or friction.

For water wave problems, which are relevant for WECs, the governing forces are usually gravity and inertia. Taking the ratio between the two, we have

$$\frac{F_{\text{inertia}}}{F_{\text{gravity}}} \propto \frac{ma}{mg} = \frac{\rho \frac{du}{dt} L^3}{\rho g L^3} = \frac{\rho \frac{du}{dx} \frac{dx}{dt} L^3}{\rho g L^3} = \frac{u^2 L^2}{gL^3} = \frac{u^2}{gL}. \quad (75)$$

Upon taking the square root we obtain the Froude number

$$\text{Froude number} \equiv \frac{u}{\sqrt{gL}}, \quad (76)$$

which will have to be satisfied at model scale as at prototype (full) scale. The scale factors for quantities of interest can be obtained by equating the Froude number for model and prototype scales. The results are shown in Table 1.

In model tests of WECs, we are normally interested in the waves or the free-surface elevations around the model, water pressures on the body or the air pressure for OWCs or flexible bag devices, forces (power take-off forces, mooring forces, wave excitation and radiation forces), motions (displacement, velocity, acceleration) of the body, flow (air flow in the case of OWCs and other devices utilising air flows, or water flow in the case of overtopping devices), and the absorbed power. It is therefore important to know the Froude scaling factors for these quantities.

Model tests of WECs are usually carried out in a wave flume or a wave basin/tank. A wave flume is long and narrow and thus more suited for studying two-dimensional problems. An example is the [UWA wave flume](#). Having a single body at the centre of a flume is equivalent to having a row of infinite number of bodies, since the side walls act as reflectors (or mirrors). This can simulate the interactions of waves with a long array of WECs. A wave basin/tank usually has comparable length and width and is therefore suited for studying three-dimensional problems such as wave interactions of a single WEC in the open sea. An example is the [Plymouth University's](#)

TABLE 1: Scale factors for Froude scaling, reproduced from [6]. Note that λ is used in the table to denote the length scale (not the wavelength).

Characteristic	Dimension	Froude
Geometric		
Length	[L]	λ
Area	[L ²]	λ^2
Volume	[L ³]	λ^3
Rotation	[L ⁰]	—
Kinematic		
Time	[T]	$\sqrt{\lambda}$
Velocity	[LT ⁻¹]	$\sqrt{\lambda}$
Acceleration	[LT ⁻²]	—
Volume Flow	[L ³ T ⁻¹]	$\lambda^{5/2}$
Dynamic		
Mass	[M]	λ^3
Force	[MLT ⁻²]	λ^3
Pressure	[ML ⁻¹ T ⁻²]	λ
Power	[ML ² T ⁻³]	$\lambda^{7/2}$

wave basin. A wave basin of course can never be an exact replica of the open sea, due to the presence of wave reflections from the boundaries. To minimise reflections, both wave flumes and basins are normally equipped with a dissipating beach at the opposite end of the wavemaker, whereas the wavemaker is normally equipped with an active absorption system (this works using essentially the same principle as the wave absorbing wall in Fig. 16). The wavemakers usually employ either piston or hinged paddles. Piston paddles are generally suited for shallow water basins, while hinged paddles are suited for deep water basins. The motion of the paddles can be programmed to generate different kinds of waves. A wave basin usually has multiple paddles, allowing the generation of waves at oblique angles and spread seas. The FloWave wave basin has a circular plan with multiple paddles all around it.

The different types of tests normally conducted in model tests of WECs include

- *Decay tests.* In these tests, the model is displaced from its mean position and released in otherwise calm water. The motion of the model is recorded. The natural period of the response can be obtained from the record and the amount of damping can be estimated from the decay rate of the response.
- *Forced oscillation tests.* In these tests, an actuator is used to force the model into harmonic oscillations in otherwise calm water.
- *Regular wave tests.* In these tests, the model is subjected to incident regular waves of various periods and amplitudes. These tests are often done to construct the frequency response

function of quantities of interest, such as displacements and forces. An example of this is shown in Fig. 24.

- *Irregular wave tests*. These are conducted to replicate a real irregular sea state.
- *Survival tests*. In these tests, we are interested in knowing how the device would respond in extreme conditions. The device can be tested in a steep irregular sea state or subjected to a focused wave group.

Example A WEC is designed to resonate at a period of 8 seconds, where it is expected to generate 100 kW of power. The target deployment location has a water depth of 20 m. If the WEC is to be tested in a wave basin with a fixed water depth of 0.8 m, what would be a suitable model scale to use for the model tests? At this scale, what would be the resonance period and the expected power output?

Answer Using the water depth to decide on the model scale, we have $0.8 : 20 = 1 : 25$. According to Froude similitude (Fig. 1), power scales as the length scale to the power of 3.5, whereas period (time) scales as the square root of the length scale. Thus, at a model scale of 1:25, the WEC will have a resonance period of $8/\sqrt{25} = 1.6$ s and produce $10^5/25^{3.5} = 1.28$ W.

8 Numerical modelling

8.1 Frequency-domain models

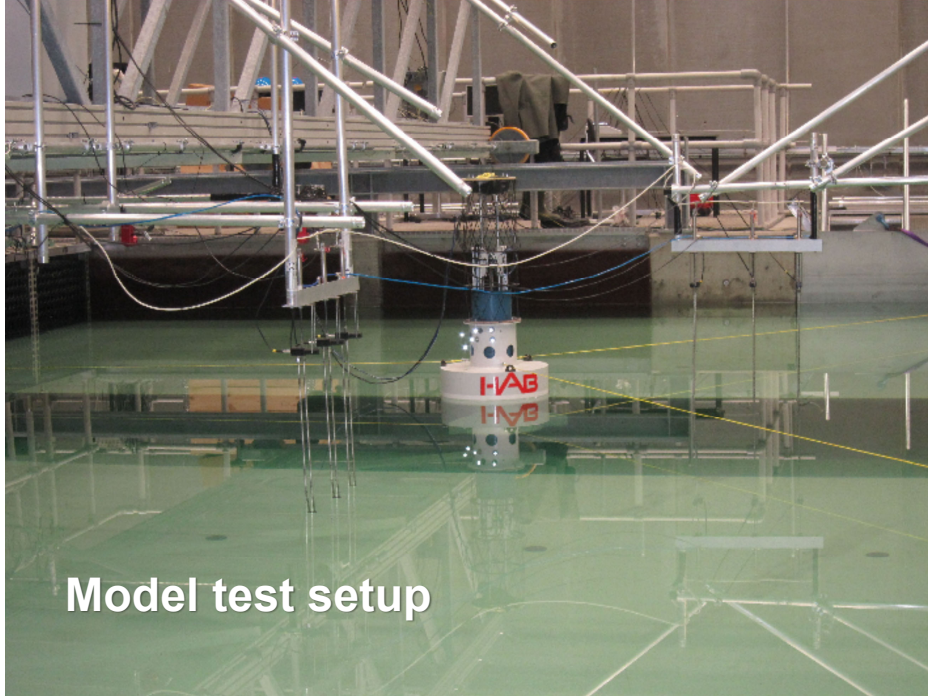
There exists a spectrum of numerical modelling techniques to model a WEC, depending on the level of fidelity and computational efficiency. In the low-fidelity and high-efficiency end of the spectrum is the linear frequency-domain model.

In a frequency-domain model, the equation of motion of the WEC is expressed in the frequency domain. For a single oscillator (a WEC oscillating in one mode), this is just the equation we have seen before (see Section 4.3):

$$\hat{F}_e(\omega) = \{R_m + R_r(\omega) + i\omega [m_m + m_r(\omega) - S_m\omega^{-2}]\} \hat{u}(\omega), \quad (77)$$

where we have used (ω) to indicate the frequency-dependent quantities. As we have seen before, this equation can be solved for the complex velocity amplitude $\hat{u}(\omega)$, from which other quantities such as the absorbed power can be calculated. For a WEC oscillating in more than one mode or for an array of multiple WECs, the equation becomes a system of linear equations, but the general form is the same.

A frequency-domain model can be solved almost instantly by a computer and is usually the first approach to use to model a given WEC. Because it is a linear model, it is necessary to assume the PTO force as linear. Losses can be modelled as a linear damping term. The hydrodynamic problem is solved based on linear potential theory. This generally gives a good approximation. Boundary element method (as implemented in e.g. **WAMIT**, **HydroStar**, **NEMOH**) is commonly used to solve



Model test setup

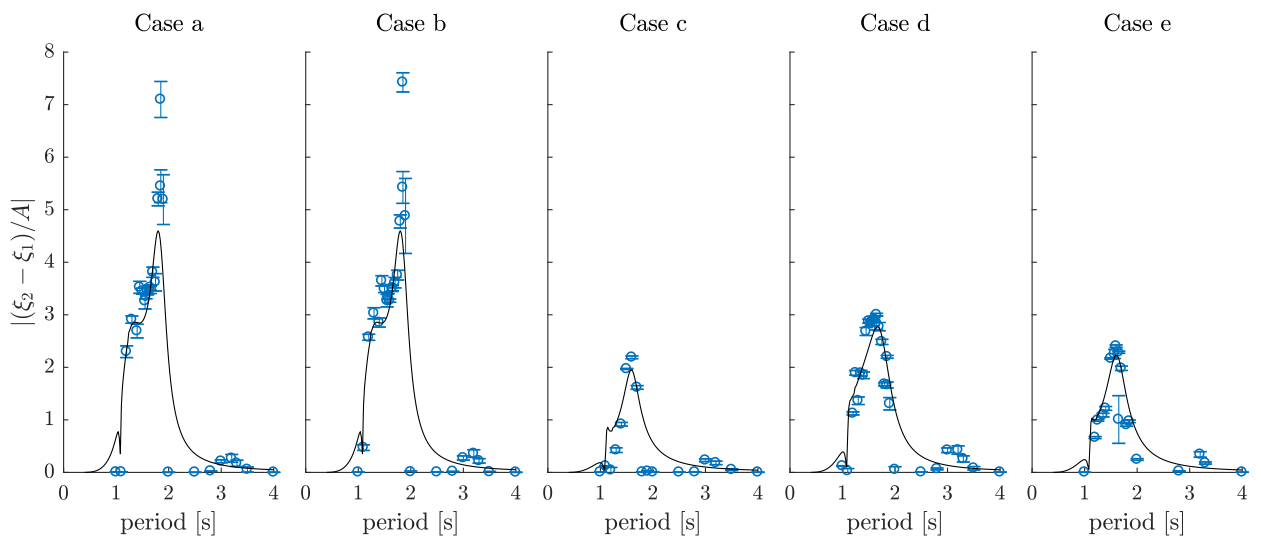
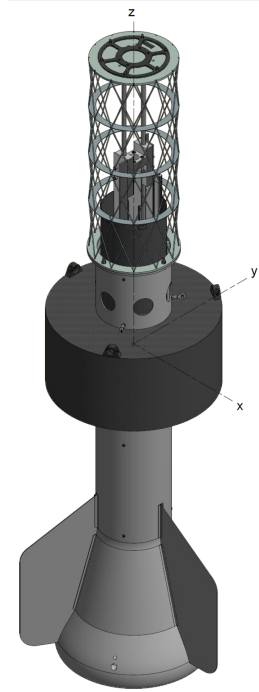


FIGURE 24: A scaled model of a WEC in a wave basin and its technical drawing. The WEC is a heaving device composed of an inner body and an outer body. Power is absorbed through relative motion between the two bodies. Plots at the bottom show comparison of the measured relative displacement between the bodies (points) and the numerical predictions (lines), from [11].

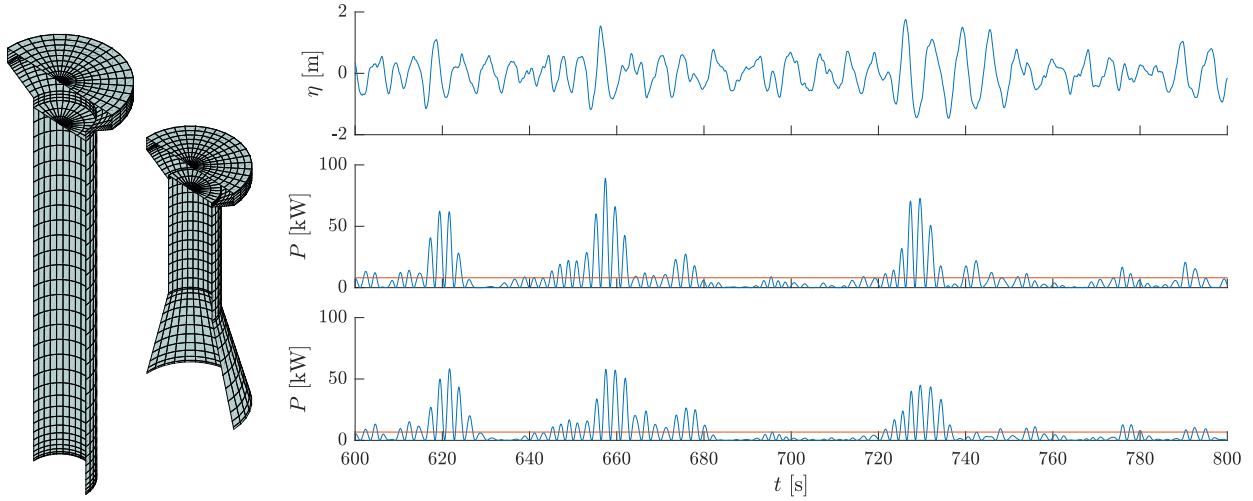


FIGURE 25: Plots on the right show the absorbed power of the two geometric variations of the WEC in Fig. 24, for the same incident irregular waves (plotted at the top). Results were obtained from a frequency-domain model. On the left are the panel models used for computing the hydrodynamic coefficients.

for the hydrodynamic coefficients (excitation force, added mass, and radiation damping terms). A panel model of the submerged geometry of the body will be needed. An example is shown in Fig. 25. The figure also shows time histories of the absorbed power calculated from a frequency-domain model.

Due to its very low computational cost, a validated frequency-domain model is useful for design optimisation, as this requires numerous computations to be made on different variations of the WEC.

8.2 Time-domain models

8.2.1 Weakly-nonlinear time-domain model

The next step from (linear) frequency-domain models is weakly-nonlinear time-domain models. For a single oscillator, it has the following form:

$$F_e(t) = [m_m + m_r(\infty)]\ddot{u}(t) + k(t) * u(t) + S_m s(t) + F_{\text{ext}}(s(t), u(t), t). \quad (78)$$

This time-domain equation (a.k.a. the Cummins' equation) is obtained by taking the inverse Fourier transform of the frequency-domain equation (77). Because of the frequency-dependence of the added mass $m_r(\omega)$ and radiation damping $R_r(\omega)$, the wave radiation force contains a convolution term $k(t) * u(t) = \int_0^t k(\tau)u(t - \tau)d\tau$, where $k(t) = \frac{2}{\pi} \int_0^\infty R_r(\omega) \cos(\omega t)d\omega$ is the radiation *impulse response function*. The convolution term is a memory term, related to the fact that waves radiated by the body in the past continue to be felt by the body at present. The other part of the radiation force is the term containing $m_r(\infty)$, the infinite-frequency added mass. In the equation, $s(t)$ is the body displacement.

As in frequency-domain models, the hydrodynamic forces are typically assumed linear. However, the time-domain formulation makes it possible to include nonlinearities, such as nonlinear PTO forces, drag, control forces, and nonlinear restoring forces. These are all contained in $F_{\text{ext}}(s(t), u(t), t)$, which is a general nonlinear force that includes the PTO force. Instead of a

linear damping term, the PTO force can be modelled more realistically in a time-domain model. An example of simulation results from a time-domain model is shown in Fig. 26. In this example, a hydraulic system is used for the PTO. A detailed model of the hydraulic PTO involving nonlinear terms is included in the time-domain model.

Time-domain models such as (78) are usually solved numerically using a time-stepping scheme, such as the Runge-Kutta methods. The convolution term, which is an integral over times past to the present, needs to be recalculated at each time step and can be time consuming to compute. It is possible to speed up computation by replacing the convolution with some approximations.

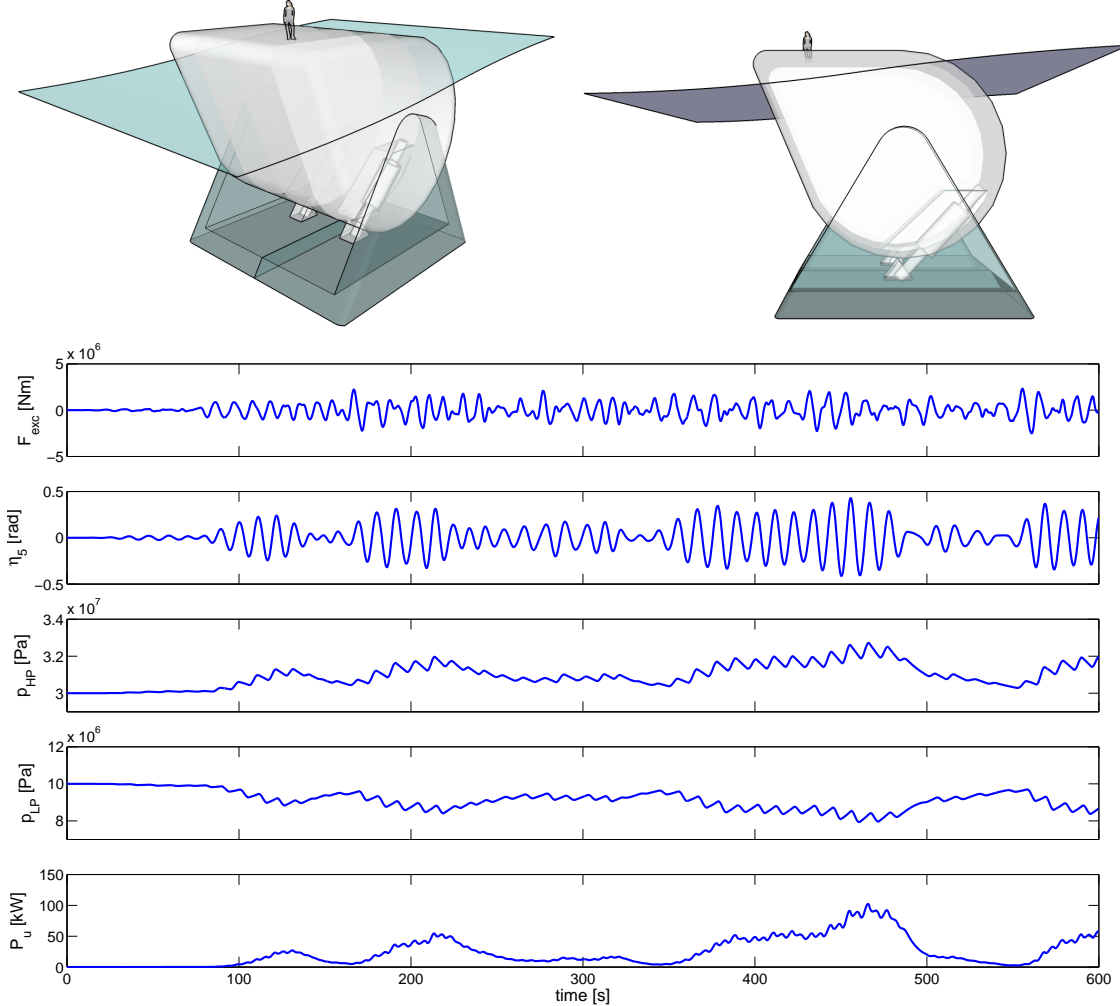


FIGURE 26: A seabed-mounted WEC similar to the Salter Duck, reproduced from [9]. The device is connected to a hydraulic PTO system. The plots show the response of the device, including the angular displacement, pressures in the high- and low-pressure accumulators, and power output, under irregular wave excitations. Results were obtained from a time-domain model.

8.2.2 Fully-nonlinear time-domain models

The preceding models (frequency-domain models and weakly-nonlinear time-domain models) are commonly used because they are computationally cheap. For WECs, we are mainly interested in the performance (power output) of the device in small to moderate wave steepness (which happen most of the time), and these models generally give good predictions for these cases. They are

also useful in parametric studies or design optimisation studies, as the effect of different design parameters on the device performance can be evaluated relatively quickly.

However, understanding certain aspects of the wave-structure interaction problems may require the use of higher-fidelity models, which can reproduce the physics of the problem more accurately but at the expense of much higher computational costs. Commonly used nonlinear time-domain models include fully-nonlinear potential flow models, which are suitable for steep but non-breaking waves, and computational fluid dynamics (CFD) models, which can capture breaking waves and account for viscous effects.

8.3 Modelling oscillating water column

Before concluding this section, let us say a few words about modelling of oscillating water column (OWC) devices. To model an OWC in the frequency domain, two approaches are possible: the massless piston model [1] and the pressure distribution model [2]. The massless piston model approximates the top surface of the water column as a massless rigid piston. Thus the models for oscillating-body WECs as given by (77) and (78) are applicable. Because the rigid piston remains horizontal at all times, this approximate model works well as long as the size of the water column is small in comparison with the wavelength, but becomes less valid for shorter wavelengths. In the pressure distribution model, no such approximation is necessary and so it is more accurate. The radiation problem is described by quantities analogous to added mass and radiation damping, but instead of force and body velocity these quantities relate dynamic air pressure and volume flow.

9 Mean power output in irregular sea

In Part 1, we discussed how to calculate the mean wave-power level at a given site, when the long-term distribution of wave heights and periods at the site is available. The mean power output of a WEC can be calculated in a similar way.

The mean power output from a given sea state characterised by a spectrum $S(\omega)$ is

$$P_a(H_s, T_p) = 2 \int_0^\infty \frac{P_a(\omega)}{|A|^2} S(\omega) d\omega. \quad (79)$$

Alternatively, if the capture width d_a (as a function of frequency) is known, then

$$P_a(H_s, T_p) = \rho g \int_0^\infty d_a v_g S(\omega) d\omega. \quad (80)$$

A table of the mean power output $P_a(H_s, T_p)$ for different combinations of H_s and T_p is often called the power matrix.

The mean power output from a wave climate, given the scatter diagram (joint probability table of wave heights and periods) at a given site, can be calculated in the same way as the mean wave-power level \bar{J} is calculated:

$$\bar{P} = \sum_{H_s} \sum_{T_p} P_a(H_s, T_p) C(H_s, T_p), \quad (81)$$

where $\sum_{H_s} \sum_{T_p} C(H_s, T_p) = 1$ (see Part 1).

The mean capture width for the entire wave climate can then be obtained as

$$\overline{d_a} = \frac{\overline{P}}{\overline{J}}. \quad (82)$$

10 Useful and interesting links

- **National Map**

The National Map has resource maps for renewable energy in Australia, including wind, hydro, wave, and tidal. For wave, click on ‘Add Data’, and go to Energy > Renewable Energy > Marine > Marine Energy Context Layers > Wave Energy Resource, where you will find different options, including ‘Wave Energy Flux’, which is the wave-power level.

- **European Marine Energy Centre (EMEC)**

The European Marine Energy Centre, established in 2003, is the world’s first and leading facility for demonstrating and testing wave and tidal energy converters. Check out the wave energy converters that have been tested there—also relevant for tidal. They also publish a set of standards and guidelines for the marine energy industry, covering a lot of aspects, from resource assessment to grid connection.

- **Wave Energy Scotland (WES)**

Wave Energy Scotland is a technology development body set up by the Scottish Government to facilitate the development of wave energy in Scotland. It implements a phase-gate approach to ensure that the most promising technologies receive maximum investment. This model has now been adopted in the [EuropeWave](#) R&D programme for wave energy technology.

- **Edinburgh Wave Power Group**

The Wave Power Group at the University of Edinburgh dates back to 1974—the year that Stephen Salter invented the ‘Duck’.

- **Johannes Falnes’ Homepage**

Similar to the Edinburgh Wave Power Group website, from the Norwegian perspective.

References

- [1] D. V. Evans. The oscillating water column wave-energy device. *J. Inst. Maths Applics.*, 22:423–433, 1978.
- [2] D. V. Evans. Wave-power absorption by systems of oscillating surface pressure distributions. *Journal of Fluid Mechanics*, 114:481–499, 1982.
- [3] J. Falnes. Research and development in ocean-wave energy in Norway. In Hideo Kondo, editor, *Proceedings of International Symposium on Ocean Energy Development*, pages 27–39, Muroran, Hokkaido, Japan, August 1993.

- [4] Johannes Falnes and Adi Kurniawan. *Ocean Waves and Oscillating Systems: Linear Interactions Including Wave-Energy Extraction*, volume 8 of *Cambridge Ocean Technology Series*. Cambridge University Press, 2 edition, 2020.
- [5] C. O. J. Grove-Palmer. Wave energy in the United Kingdom: A review of the programme June 1975 - March 1982. In H. Berge, editor, *Proceedings of the 2nd International Symposium on Wave Energy Utilization*, pages 23–54, Trondheim, Norway, 1982.
- [6] B. Holmes. *Tank testing of wave energy conversion systems*. The European Marine Energy Centre, Orkney, UK, 2009.
- [7] J. M. J. Journée and W. W. Massie. *Offshore Hydromechanics*. Delft University of Technology, 2001. Available from <http://www.shipmotions.nl/DUT/LectureNotes/OffshoreHydromechanics.pdf>.
- [8] A. Kurniawan, J. Hals, and T. Moan. Assessment of time-domain models of wave energy conversion systems. In *Proceedings of the 9th European Wave and Tidal Energy Conference*, Southampton, 2011.
- [9] A. Kurniawan, E. Pedersen, and T. Moan. Bond graph modelling of a wave energy conversion system with hydraulic power take-off. *Renewable Energy*, 38(1):234–244, 2012.
- [10] Adi Kurniawan. *Modelling and geometry optimisation of wave energy converters*. PhD thesis, Norges teknisk-naturvitenskapelige universitet, 2013.
- [11] Adi Kurniawan, Matthias Grassow, and Francesco Ferri. Numerical modelling and wave tank testing of a self-reacting two-body wave energy device. *Ships and Offshore Structures*, 14(sup1):344–356, 2019.
- [12] S. H. Salter. Looking back. In J. Cruz, editor, *Ocean Wave Energy: Current Status and Future Perspectives*. Springer, 2008.
- [13] WAMIT. *User Manual*. WAMIT, Inc., Chestnut Hill, MA, 2016. Version 7.2.